ANKARA UNIVERSITY
GRADUATE SCHOOL OF NATURAL AND APPLIED SCIENCES

MASTER OF SCIENCE THESIS

REAL TIME MONITORING OF INTRARENAL PRESSURE FOR ENDOUROLOGICAL PROCEDURES

Mahmure Gül ŞAKI

DEPARTMENT OF BIOMEDICAL ENGINEERING

ANKARA
2021

ABSTRACT

Master of Science Thesis

REAL TIME MONITORING OF INTRARENAL PRESSURE FOR ENDOUROLOGICAL PROCEDURES

Mahmure Gül ŞAKI

Ankara University
Graduate School of Natural and Applied Sciences
Department of Biomedical Engineering

Supervisor: Prof. Dr. Hilal GÖKTAŞ

Co-Supervisor: Assoc. Prof. Dr. Mehmet İlker GÖKÇE, MD

Endourology refers to a specific area of urologic surgery, where small internal endoscopes and instruments are used to view and perform surgery on the urinary tract. In this thesis study, we aimed to measure the intrarenal pressure during endourological procedures. Since the increase in intrarenal pressure has potential to cause perioperative complications, it is an important parameter to be monitored during the operation. Saline solution is used for irrigation during endourologic procedures. The irrigation is crucial to maintain a clear image inside the urinary tract, while transporting the emerging stone dust and fragments. Increase in the intrarenal pressure can trigger pyelovenous reflux and therefore the bacteria or other endotoxins in the collecting system may be transferred to the systemic blood flow. This may result in bacteremia and septic complications which may lead to prolonged antibiotic therapy, intensive care unit admission, and even death. To prevent the mentioned complications, the intrarenal pressure should be kept below 40 cmH_2O. In this study, a pressure sensor was integrated with ureteral catheter and ureteral access sheath to screen real-time pressure value in different endourological procedures.

September 2021, 63 pages

Key Words: Intrarenal pressure, Urethral catheter, Percutaneous nephroscopy, Endourology

ÖZET

Yüksek Lisans Tezi

ENDOÜROLOJİK İŞLEMLERDE GERÇEK ZAMANLI İNTRARENAL BASINÇ ÖLÇÜMÜ

Mahmure Gül ŞAKI

Ankara Üniversitesi
Fen Bilimleri Enstitüsü
Biyomedikal Mühendisliği Anabilim Dalı

Danışman: Prof. Dr. Hilal GÖKTAŞ

Eş Danışman: Doç. Dr. Mehmet İlker GÖKÇE, MD

Endoüroloji, küçük dahili endoskopların ve aletlerin idrar yolunda ameliyatı görüntülemek ve gerçekleştirmek için kullanıldığı belirli bir üroloji uzmanlığını ifade eder. Bu tez çalışmasında endoürolojik işlemler sırasında intrarenal basıncı ölçümü amaçlanmıştır. İntrarenal basınçtaki artış perioperatif komplikasyonlara neden olma potansiyeline sahip olduğundan operasyon sırasında önemli bir parametre olarak izlenmelidir. Ameliyatlarda irrigasyon için salin solüsyon kullanılır. İrrigasyon sıvısı, ortaya çıkan taş tozu ve parçalarını taşırken idrar yolunun içinde net bir görüntü sağlar. İntrarenal basınçtaki artış piyelovenöz reflüyü tetikleyebilir ve bu nedenle toplama sistemindeki bakteri veya diğer endotoksinler sistemik kan akışına aktarılabilir. Bu, uzun süreli antibiyotik tedavisine, yoğun bakıma yatışa ve hatta ölüme yol açabilen bakteremi ve septik komplikasyonlara neden olabilir. Bahsedilen komplikasyonları önlemek için intrarenal basınç 40 cmH_2O'nun altında tutulmalıdır. Bu çalışmada, farklı endoürolojik prosedürlerde gerçek zamanlı basınç değerini taramak için üreteral kateter ve üreteral girişim kılıfı ile bir basınç sensörü entegre edildi.

Eylül 2021, 63 sayfa

Anahtar kelimeler: Intrarenal basınç, Üretral kateter, Perkütan Nefroskopi, Endoüroloji

ACKNOWLEDGEMENTS

I would like to extend my heartiest thanks to all those who provides me immense help and guidance during my master degree studies.

I would like to express my sincere gratitude to my supervisor Prof. Dr. Hilal Göktaş and my co-supervisor Assoc. Prof. Dr. Mehmet İlker Gökçe, MD for providing valuable academic guidance in my thesis study.

I am thankful to entire members of Mega Özel Health; especially my bosses Dr. Osman Tunç, MD and Dr. Celal Alp Tunç; my managers Gülay Gülşen Erenç, Murat Çorum and Mert Nizamoğlu for their guidance, suggestions, encouragement and insightful support throughout the duration of my study.

Finally, I am very grateful to my beloved family; my father Yüksel Şakı, my mother Nejla Şakı and my brother Mert Şakı who are always around and encouraging me. It would not be easy to start and achieve my degree of Master of Science without their support and understanding.

M. Gül ŞAKI
Ankara, August 2021

INDEX

SYMBOLS AND ABBREVIATIONS

°C	degree of Celsius
cmH_2O	centimeter of water
mmHg	milimetres of mercury

List of Abbreviations

IRP	Intrarenal Pressure
PCNL	Percuatenous Nephrolitotomy
RIRS	Retrograde Intrarenal Surgery

LIST OF FIGURES

LIST OF TABLES

1. INTRODUCTION

Endourological upper tract treatments such as Percutaneous nephrolithotomy (PCNL) and Retrograde intrarenal surgery (RIRS) constitute the main procedures of active renal stone management. The new techniques, innovations and instrumentation open new treatment options in endourology. One of the main aim of researches and biomedical applications is the improvement of the image quality by achieving better irrigation flow and irrigation pressures (Tokas, Herrmann, et al., 2019). During different endourological procedures, there are possible ways to maintain lower pressure values even working with high irrigation flow (Alsmadi et al., 2018; Rawandale-Patil et al., 2019). During the procedures, the intrarenal pressures (IRPs) should be under control. IRPs below the 40 cmH_2O should be maintained to avoid post-op complications (Monga et al., 2004).

In literature, there have been nine different studies that identified the IRPs during the Retrograde Intrarenal Surgeries (Tokas, Skolarikos, et al., 2019). The in-vitro studies; in vitro human cadaveric (Rehman et al., 2003) and in vitro mini-pig (Schwalb et al., 1993) was performed. In longest duration of measurement, the study of Schwalb et al. (1993) on pigs, was shown that prolonged exposure which is longer than 45 min, the intrarenal pressure is exceeded 200 cmH_2O. In addition, the high-pressure value was associated with inflammation and renal scarring.

In-vivo studies on RIRS; in human (Cai et al., 2012; Doizi et al., 2021; Jung et al., 2008; Schwalb et al., 1993; Shao et al., 2012), and in-vivo porcine study (Caballero-Romeu et al., 2018) by using semi-rigid and flexible ureteroscopes (URS) was also performed. The irrigation pressures reported are 68–272 cmH_2O, where the IRPs reported 8.27–199.35 cmH_2O depending on the irrigation pressure. These studies also show that the endourological instruments should have inflow and outflow channels that solve image quality and intrarenal pressure problem by continuous flow property of the channels (Michel et al., 2008; Suh et al., 2010). The continuous flow ureteroscopes provide 100 times higher flow capacity while preserving intrarenal pressure during procedure (Michel et al., 2008). In the recent study of Doizi et al. (2021), a digital sensor was used as novel procedure real time, continuous monitoring of IRP measurement. The intrapelvic pressure was recorded as mean baseline intrarenal pressure was 6 cmH_2O. The mean intrarenal pressure with the use of on demand forced irrigation during laser lithotripsy was 115.3 cmH_2O. The highest-pressure peaks recorded during lithotripsy ranged from 289.3 to 436.9 cmH_2O (Doizi et al., 2021).

The other procedure of endourology, the PCNL, is utilized by percutaneous nephroscope for larger kidney stones. Since the introduction of PCNL in 1976, it is preferred for renal stones larger than 2 cm in diameter (Fernstrom & Johansson, 1976; Turk et al., 2016). The size of the instrument changes the name of the PCNL. The sizes of 26–30 Fr is named as the standard PCNL where 20 Fr smaller instrument is called mini-PCNL (Lahme et al., 2001). As an improvement in 2010, the 1 mm scope size with 11 or 13 Fr sheaths is introduced with name ultra-mini-PCNL (Desai et al., 2013).

The IRPs during PCNL have been identified in literature (Theodoros Tokas, 2019). The in-vivo studies were; in-vivo human (Alsyouf et al., 2018; Guohua et al., 2007; Saltzman et al., 1987; Tepeler et al., 2014; Troxel & Low, 2002; Zhong et al., 2008) and an in vivo porcine model (Loftus et al., 2018) was performed. Standard PCNL and mini-PCNL were used in studies, the IRPs ranged between 3.0–41.21 cmH_2O in PCNL with sheath sizes ranging 26–34 F. The 26-22 Fr PCNL have given results as 13–50 cmH_2O. In one of percutaneous nephrolithotomy study, intrarenal pressures were greater than 40.8 cmH_2O (Theodoros Tokas, 2019).

An in-vitro human kidney model (Low, 1999), an ex-vivo human cadaveric model (Landman et al., 2002) and in vitro artificial models (Goble & Hammonds, 1987; Mager et al., 2015) was performed. In study of Mager et al. (2015), they were compared 15 F, 16.5 F, 21 F and 26 F conventional PCNL systems. With 16.5 F, 21 F, and 26 F PCNL systems, the continuous low pressure under 25 cmH_2O is obtained even the irrigation flow pressure rose to 140 cmH_2O (Mager et al., 2015).

The increase in IRP might have cause complications due to absorption of bacteria or endotoxin to the systemic circulation. Even at low IRP during PCNL, absorption of endotoxin or bacteria containing irrigation fluid may occur. Systemic absorption of irrigation fluid containing endotoxin or bacteria may lead to urosepsis or fever after PCNL as post-op complications (Troxel & Low, 2002). Intrapelvic pressure greater than 30 mmHg, which is equal to 40 cmH_2O, has been shown to result in pyelovenous lymphatic backflow, pyelotubular backflow and forniceal rupture (Tokas, Herrmann, et al., 2019). In the study of Hinman (1928), pyelovenous backflow occurred at canines at renal pressures above 40-47 cmH_2O. Additional studies showed that pyelovenous backflow may also occur at pressures as low as 13-27 cmH_2O. According to these studies, during clinical practice maintaining IRP of less than 40 cmH_2O is recommended (Kukreja et al., 2002; Stenberg et al. 1988).

There is no study in the literature regarding the application of ureteral catheter-pressure sensor and ureteral access sheath-pressure sensor combination, which is important in controlling the effect of irrigation flow on intrarenal pressure. In in-vivo study of Doizi et al. (2021), they were used digital sensor only for RIRS and they were inserted sensor through the instrument channel. The current studies show, there is lack of proper designed disposable with sensor channel and executed human studies. Therefore, in this study, pressure sensor was combined with ureteral catheter and ureteral access sheath for the first time, to be used in endourological procedures, especially percutaneous nephrolithotomy, to prevent complications.

2. LITERATURE SURVEY

2.1 Urinary System

The urinary system filters blood where urea is carried then creates urine as a liquid waste by-product. Urea is produced after protein contained foods are broken down (Anonymous, 2020). The system keeps water and chemicals, such as sodium, potassium in balance. The urinary system include the kidneys, ureters, bladder and urethra (Standring, 2008b).

2.1.1 Kidney

The kidney sustains the body homeostasis by eliminating excess body fluid, salts, foreign substances and byproducts of metabolism. The organ regulates blood osmolarity, pH, blood volume and blood pressure and produces hormones (Elbadawi, 1996; Fowler et al., 2008).

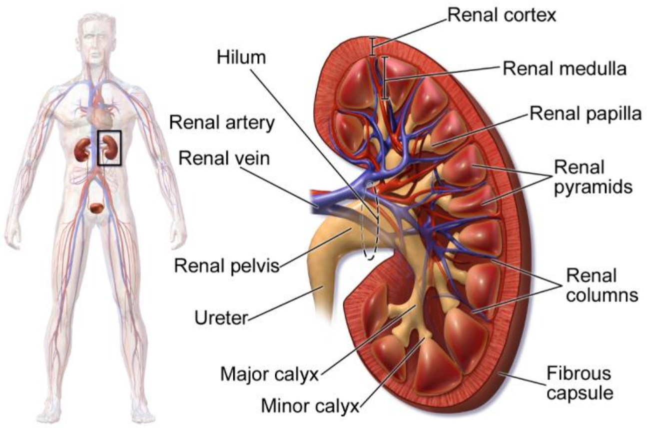

Figure 2.1 Kidney anatomy (Medical, 2014)

The kidneys are bilateral organs placed in the upper left and right abdominal quadrants retroperitoneally. They are between the transverse processes of T12-L3 vertebrae. Typically, the left kidney positioned more superior than the right due to location of the liver and the stomach (Standring, 2008b).

The kidney is surrounded by a thick layer of adipose tissue which called perirenal fat. The layer protects the organ. The renal fascia is a connective tissue that hold the organ in place. In the adult, each kidney is 12 cm long, 6 cm wide and 3 cm thick, approximately. It is bean like shaped with a recess on the medial side that called the hilum. The hilum is the beginning of the renal pelvis. The renal pelvis is where the ureter and renal vein leave the kidney; also the renal artery enters the kidney (Hickling et al., 2015; Standring, 2008b).

The renal cortex is outer surrounding of the renal medulla. The renal medulla forms of a series of renal pyramids. Renal pyramids are striated due to presence of blood vessels and straight tubular structures. The pyramids are ended in renal papillae where the kidney pelvis is connected. The renal pelvis is a cavity of urine effusion. The calyces are peripheral to renal pelvis and collects urine from each pyramid (Anonymous, 2009; Hickling et al., 2015).

The renal cortex is enlarged to place between adjacent pyramids that called renal columns and forms functional parenchyma of kidney. In parenchyma, millions of nephrons are collected urine from afferent arteriole. An afferent arteriole is connected to renal corpuscle of parenchyma that consist of capillaries called glomerulus (Anonymous, 2009).

2.1.2 Ureter

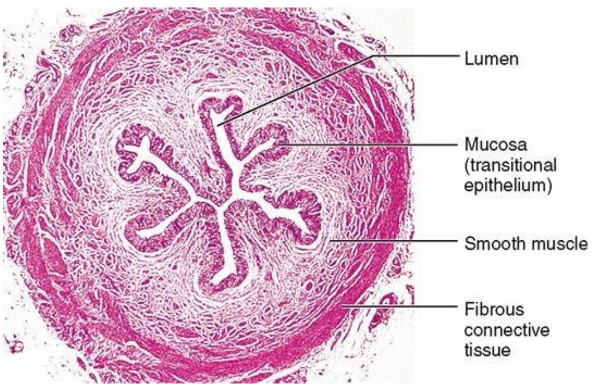

Figure 2.2 Ureter structure (Anderson 2012)

The renal pyramids are the functional tissue that create urine. Whereas, the calyces are the beginning of the ureter. The urine is transported by ureter from renal pelvis to bladder. The ureters are approximately 25 cm long in narrow tube form, lies down on the posterior abdominal wall. They reaches the posterior inferior surface of bladder (Anderson, 2012).

The outer, middle and inner layer are structured the ureter. The fibrous outer layer is surrounded by the middle muscular layer. The muscular coat of middle layer has outer longitudinal smooth and inner circular muscle that drive urine downward (Anderson, 2012; Standring, 2008b). Approximately, every 10-15 seconds, a couple amounts of urine are transported into the bladder. The inner layer is mucosa which is epithelium that is also lining of the bladder and renal pelvis. The mucosa secretes mucus and protects the surface of the cells (Hickling et al., 2015).

2.1.3 Urinary Bladder

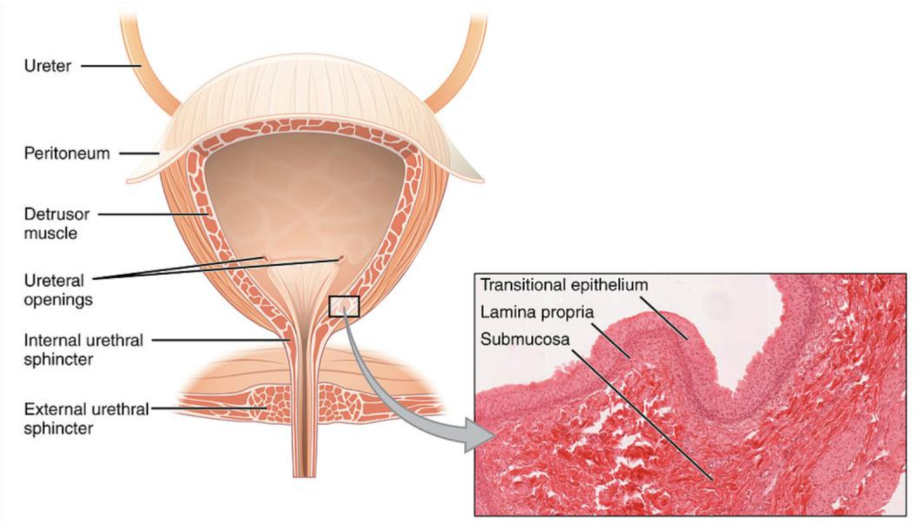

Figure 2.3 Schematic representation of urinary bladder (Weblogographic.com, 2019)

The urinary bladder is located in pelvic cavity, in lower abdomen and functions as temporary storage of urine. The inner layer is mucous membrane of epithelium that continues from ureters. The rugae structure in mucosa allows the bladder to expand when urine accumulated inside. A typical healthy adult bladder can store urine for 2-5 hours. The submucosa is the second connective tissue layer with elastic fibers, supports the mucosa. The urine is expelled from bladder by contraction of muscularis, the smooth muscle layer. The outermost layer is parietal peritoneum that consists of fibrous connective tissue (Macarak & Howard, 1999).

The bladder trigone is formed by 2 ureteral and 1 urethra openings. The ureteral openings are covered by small flaps of mucosa to prevent urine from going back into ureters and kidneys. These openings are called orifice. Adding to this, there is urethral sphincter that is created by detrusor muscle (Standring, 2008a).

2.1.4 Urethra

The last station of the urinary system is urethra. The transition of urine from urinary bladder to outside is occurred (de Groat & Yoshimura, 2001). The cross-sectional structure consists of mucosal transitional epithelium and smooth muscle fibers (Standring, 2008a).

The beginning of the urethra is surrounded by internal urethral sphincter, a smooth muscle. Contrary, at the end is encircled by skeletal muscle that called external urethral sphincter. The two sphincters control the urine flow along the urethra with brain signals. In female, the urethra is shorter than males in size of 3-4 cm. The external urethral orifices open to opening of the vagina (Chung, 2012; Park et al., 1997).

In males, the urethra is about 13-20 cm long with three parts where semen and urine are transported. The first part is called prostatic urethra and passes through the prostatic gland. This layer continues with membranous urethra and spongy urethra. The membranous urethra is surrounded by striated muscle known as the external urethral sphincter and in 2-2.5 cm long. The last portion, spongy urethra is the longest region, extends along the external orifice, penis and the meatus enter to outside at the tip of it (Chung, 2012; Park et al., 1997; Standring, 2008a).

2.2 Urinary Stone Disease

Urinary stone disease patients with ureteral stones present with symptoms of fever, vomiting and loin pain in usual. In some of the cases renal stones might be asymptomatic (Wimpissinger et al., 2007). The main biochemical examinations include blood cell count, uric acid, calcium, creatinine and electrolytes. If urinary tract infection is existed for patient, C-reactive protein also should be examined (Skolarikos et al., 2015).

Ultrasound is preferring as the primary imaging tool for diagnosing that can identify stones located in the urinary tract. The sensitivity and specificity in ultrasound imaging, are 19–93% and 84-100%, respectively (Ray et al., 2010; Smith-Bindman et al., 2014).

2.2.1 Urinary Stone Disease Epidemiology and Aetiology

Stone incidence depends on ethnic, genetic factors, dietary, geographical and climatic. Hypertension, type 2 diabetes, obesity and coronary heart disease risk factors are associated with nephrolithiasis (Hamano et al., 2005; Ramey et al., 2004).

According to epidemiological surveys have been reviewed the countries with a high standard of life, like Sweden, Canada or the United States of America, the urinary stone prevalence is higher than 10% (Trinchieri, 1996). In the United Kingdom, the lifetime prevalence of urinary stones increased by 63% in 10 years, between 2000 and 2010, according to data of the National Health and Nutrition Examination Survey (Turney et al., 2012). In Western countries, due to the improved clinical diagnostic procedures, nutritional and environmental changes, the incidence of urinary tract stones are increasing. In some developing countries in tropical regions, prevalence showed parallel results of Western countries, especially high in warm months (Trinchieri, 2008).

More frequently children patient with upper urinary tract stones were correlated with metabolic disturbances more than urinary tract infections or abnormalities (Coward et al., 2003). Nutritional risk factors for urinary stone diseases were differed by sex and age of the patient. In younger women, reduced risk of stone formation was correlated with dietary calcium and fluid intake. However, sucrose and animal protein enhanced the risk of urinary stone (Curhan et al., 2004). In older patients, there were no relation between stone formation and dietary calcium. Nevertheless, intakes of potassium, magnesium and fluid reduced the risk, whereas intake of vitamin C enhanced (Taylor et al., 2004; Trinchieri, 2008).

2.2.2 Urinary Stone Formation

Kidney stones are in size between a grain of a pearl to sand. The formation of a stones starts from crystal nucleation. Then, continues to the formation and growth phases of the developing stones (Khan & Hackett, 1993; McKee et al., 1995). The stone formation has been identified as two mechanisms in multistep for initial development of stone. The main differences between mechanisms are the places of the initial formation. Regardless of the mechanism, the nucleation and crystal growth are necessary for the initiation and stone development of any kinds (Khan et al., 2016; Robertson et al., 1971).

Nucleation is a process of accumulation of solute molecules scattered in a solvent. Stone formation is caused by an abnormal combination of factors, which influence the thermodynamic driving force. It is called supersaturation. The principal of the thermodynamic driving force is the degree of supersaturation of the fluid within which initiation occurs (Finlayson & Reid, 1978; Khan et al., 2016).

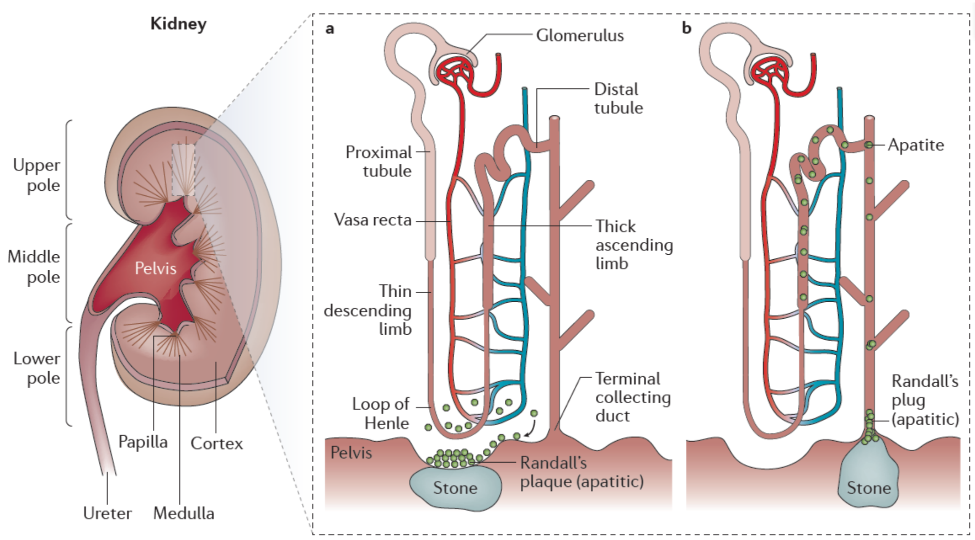

Figure 2.4 Urinary stone formation mechanisms: “free particle” (a), and “fixed particle” (b) mechanisms (Khan et al., 2016)

One of the mechanisms is called “free particle”, in which uric acid, calcium phosphate or cystine crystals form Randall’s plugs in renal tubules (Figure 2.4.a). After the Randall’s plugs formation, it moves with the urine, cluster and plug the terminal collecting ducts. The plugs are subjected to the pelvis urine while calcium oxalate crystals depositing on the calcium phosphates plug to form calcium oxalate kidney stones by encrustation (Finlayson & Reid, 1978; Khan et al., 2016; Kok & Khan, 1994).

“Fixed particle” mechanism is the second proposed formation. The stone is formed on calcific plaques on the surface of the papillary (Khan & Canales, 2015). The plaques are named Randall’s plaques and development is started with supersaturation of calcium phosphate crystal formation and deposition in the renal tubules. It is occurred at the beginning of the collecting duct system and at the end of the loop of Henle (Figure 2.4.b). In that point, two different pathways have been proposed that supersaturation is occurred in the basement membrane of the loop of Henle and initiated the plaque formation (Step 2) (Figure 2.5.a). In alternative, crystal formations may occur in the renal tubules (Step 3) and calcium phosphate crystals translocate into the interstitium (Step 4). Another possibility, the renal epithelial cell is produced reactive oxygen species when exposed to calcium oxalate and calcium phosphate; osteogenesis is happened. Epithelial cells are produced matrix vesicles (Step 5) which is continued by their calcification (Step 6) (Khan et al., 2016).

When calcium phosphate crystals have been accumulated in the collecting ducts or basement membrane of the loop of Henle; mineralization continues (Figure 2.5.b). Membranous vesicles and collagen fibers are calcified (Step 1). The subepithelial plaque is established when mineralization front arrives the renal papillary surface (Step 2). The papillary surface epithelium is disrupted and plaques are ruptured. Explosion of the calcium phosphate crystals to the pelvic urine is occurred (Step 3-4). Urinary macromolecules are accumulated on the subjected calcium phosphate crystals. The deposition of calcium oxalate on calcium phosphate base is promoted (Step 5) (Khan et al., 2016).

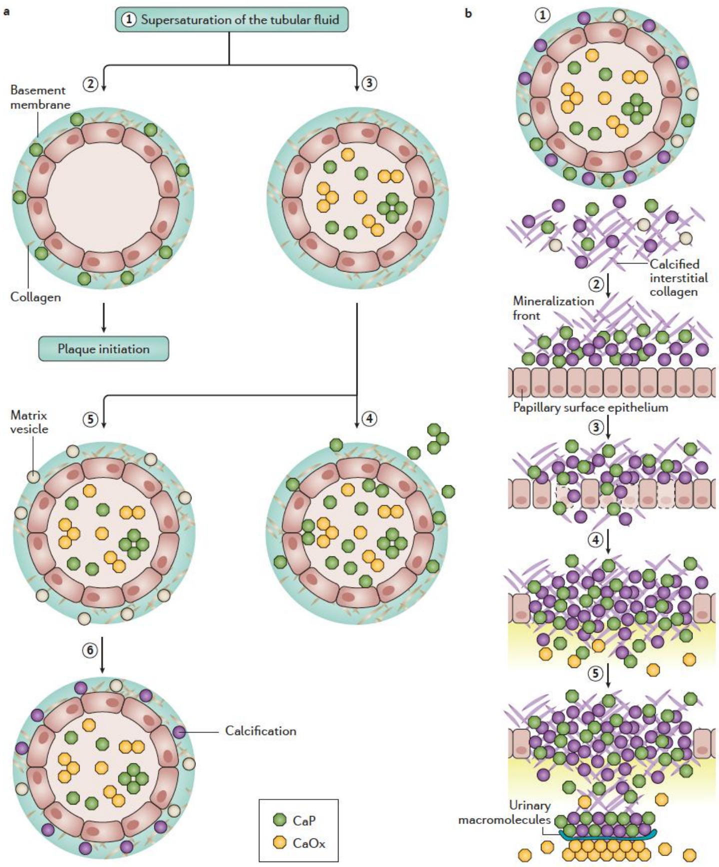

Figure 2.5 Randall’s plaque (a) and calcium oxalate (b) stone formation (Khan et al., 2016)

2.2.3 Urinary Stone Classifications

Stones can be classified by location, size, X-ray characteristics and etiology of formation (Hesse et al., 2003; Kim et al., 2007; Leusmann et al., 1990). A CT can identify inner structure, density and composition of stones that effect the treatment decision of surgeon. Stones varies according to mineral composition which classified by the kidney-ureter-bladder radiography (Kim et al., 2007).

Table 2.1 Stone classifications (Turk et al., 2016)

Classification Factors		
Stone size	<5 mm 5-10 mm 10-20 mm >20 mm	
Location	Upper calyx Middle calyx Lower calyx Renal pelvis Upper ureter Middle ureter Distal ureter Urinary bladder	
X-ray	Radiopaque	Calcium oxalate dihydrate Calcium phosphates Calcium oxalate monohydrate
	Poor radiopacity	Magnesium ammonium phosphate Cystine Apatite
	Radiolucent	Uric Acid Xanthine Ammonium urate 2,8-Dihydroxyadenine Drug Stones
Aetiology	Non–infection stones	Calcium oxalate Calcium phosphate including brushite and carbonate apatite Uric acid
	Infection stones	Magnesium ammonium phosphate Ammonium urate Carbonate apatite
	Genetic causes	Drug Stones Cystine Xanthine 2,8-Dihydroxyadenine

2.3 Urinary Stone Disease Treatments

2.3.1 Medical Expulsive Treatment (MET)

The urinary stones, smaller than 6 mm, can pass the urinary tract spontaneously. However, medical expulsive treatments increase the chance of passage and stone-free-rate. α-Adrenergic receptor antagonists, mainly tamsulosin is used, and calcium channel blockers are demonstrated as an powerful medical expulsive therapy. These drugs increase the stone passage by dilating the distal ureter.

The meta-analysis of Hollingsworth et al. (2006), medical expulsive treatments with calcium channel inhibitors or a-blockers or reducing the time on stone expulsion. The stones pass more easily in the patients with less pain episodes than whose not having MET. Also, the treatment reduces the need of analgesics due to less pain episodes (Hollingsworth et al., 2006; Seitz et al., 2009).

According to meta-analysis, MET relies on generic drugs, like doxazosin or Tamsulosin, which are inexpensive. Surgical management of stones such as Retrograde Intrarenal Surgery (RIRS), Extracorporeal Shockwave Lithotripsy (ESWL) or Percutaneous Nephrolithotomy (PCNL) are costly, due to investment for ureteroscopy, shock-wave lithotriptor or percutaneous nephroscope (Hollingsworth et al., 2006).

The MET might be supportive treatment option after ESWL, RIRS or PCNL. However, the treatments should be ceased in case of pain, infection or disconcertion of kidneys' function (Hollingsworth et al., 2006).

2.3.2 Laparoscopic or Open Surgery

Laparoscopic or open or surgery are possible treatment options, in case other treatment modalities are not suitable. The process has innovated from open surgical lithotomy to minimally invasive endourological surgeries over 30 years. The indications for laparoscopic or open stone surgery are limited. However, in case of endourologic procedures have been performed without success, the surgery can be chosen especially for centrally located renal stone mass (Alivizatos & Skolarikos, 2006; Turk et al., 2016).

2.3.3 Extracorporeal Shockwave Lithotripsy (ESWL)

Extracorporeal Shockwave Lithotripsy (ESWL) is a non-invasive transfer of high energy acoustic waves for fragmenting the urinary stones. The electromagnetic, electro-hydraulic or other types of energy sources is created a shockwave. The shockwaves are focused on the urinary stones by acoustic lens. When the wave passes through the calculus, energy is delivered and stone is fragmented (Ordon et al., 2014; Scales et al., 2014).

The number of shockwaves can be applied at different sessions. It depends on the types of shockwave power and lithotripter (Ordon et al., 2014). In studies of Pace et al. (2005) and Semins et al. (2008), best clinical practice in shockwave lithotripsy have success by lowering the frequency. The frequency is decreased from 120 to 60–90 shockwaves/min and frequency are set to 1.0–1.5 Hz to improve the stone-free-rate.

ESWL have success in good rate of stone-free for stones smaller than 2 cm, except for lower pole stones which are more suitable for endourology, RIRS and PCNL. In addition, the shockwave resistant stones, like brushite, cystine and calcium oxalate monohydrate and is not suitable for ESWL, they are resistant to fragmentation (Wignall et al., 2008). In addition to location and stone's composition limitations, ESWL may requires repeated treatments to match the effect of endourological procedures. Compared to PCNL and RIRS, there are less complications with ESWL which have higher satisfaction scores, faster return to work and shorter recovery times (Pearle et al., 2001). ESWL also has a low complication profile, the rate for urinary tract infection and steinstrasse is 2% and 5%, respectively. The steinstrasse refers to multiple small ureteric stones, seen aligned in the ureter (Muller-Mattheis et al., 1991).

The contraindications of ESWL are pregnancy, uncontrolled urinary tract infection and severe obesity, bleeding diatheses, anatomical obstruction distal to the stone and severe skeletal malformations (Turk et al., 2016). Deep sedation or general anesthesia is commonly used during procedure. The success of ESWL is determined after 1-3 months. The small residual fragments that the size is smaller than 4 mm are considered to pass ureter. The patients with these stones referred as stone-free. The medical expulsive therapies after ESWL might increase expulsion rate, rate of stone-free and reduce additional analgesic requirements (Pearle et al., 2001).

2.3.4 Retrograde Intrarenal Surgery (RIRS)

The technical availabilities and improvements of wide range of disposables are increased the usage of ureteroscopies (URS). Miniaturization of endoscopes and improved optical quality in both flexible and rigid URS resulting in shorter operation times (Binbay et al., 2010; Wendt-Nordahl et al., 2011). Moreover, digital flexible URS (f-URS) demonstrates brief operating times because of the image quality improvement (Binbay et al., 2010).

URS have lower rate of stone-free for stones greater than 2 cm. Also, the harder stones composed of brushite, cystine or calcium oxalate monohydrate are more effective for URS. A systematic review of renal stones which are greater than 2 cm showed stone-free-rate of 91% with 1.45 procedures/patient (Binbay et al., 2010; Geraghty et al., 2015).

Rigid or flexible URS might be used through the ureters depend on patients' anatomy (Figure 2.6). Ureteroscopies have retrograde passage of an endoscope from the urethra towards the kidney and ureter. When scope reach to the stone, other instruments, such as guidewires, balloon dilators, laser fibres and baskets can be delivered from scope's working channel (Wignall et al., 2008).

The non-invasive ureteroscopy procedures require general or spinal anesthesia to decrease the pain and visceral response to dilation (Cybulski et al., 2004). The fluoroscopic equipment should be ready in the operation room due to safety reasons. During procedure, placement of a safety guidewire is highly recommended. In case of difficulty during insertion of a f-URS, using rigid URS firstly might be helpful for optical dilation (Dickstein et al., 2010). A double J (JJ) stent insertion before the operation is offered also as an alternative to dilation to obtain ureteral access (Ge et al., 2016; Pace et al., 2017). Ureteral access sheaths (UASs) can be inserted by a guidewire to obtain easy access for upper urinary tract. The inner diameter of the sheath is available from 9F and thicker. Use of a hydrophilic-coated UAS reduces intrarenal pressure, also improves operation vision by sustaining the continuous flow of irrigation fluid (L'Esperance J et al., 2005; Stern et al., 2007). As a result, it reduces operating time. RIRS is removal of stones completely from urinary tract and they can be extracted by endoscopic baskets or forceps (Santiago et al., 2017). The nitinol endoscopic baskets might be used for f-URS (Bach et al., 2008). The holmium yttrium-aluminum-garnet (Ho:YAG) and Thulium fiber laser (TFL) systems are preferred method of lithotripsy. The fibers of the systems are inserted through the working channel with different diameter options in micron and use for fragmentation and dusting of all kind of stones (Leijte et al., 2008; Pierre & Preminger, 2007).

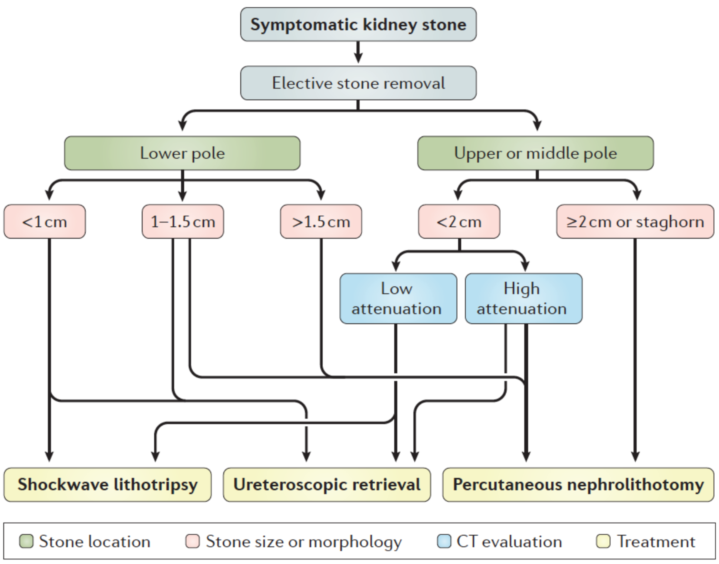

Figure 2.6 Algorithm for the most common approaches for treatment options (Khan et al., 2016)

Rigid URS are used for distal ureteral stones, whereas f-URS are used to reach each of the calyx by chance of their manoeuvre and deflection ability up to 275 degree. The complications rate of RIRS is 9–25% and mostly minor complications that not require intervention (Geavlete et al., 2006; Perez Castro et al., 2014).

A meta-analysis of seven randomized controlled trials which is involved more than 1200 patients have showed that RIRS have higher rate of stone-free and less need for second treatment than ESWL did (Aboumarzouk et al., 2012). As in the Table 2.2, for urinary stones smaller than 1 cm in size, ESWL and RIRS are considered as primary therapy. For urinary stones greater than 1 cm in size, RIRS result in higher stone-free rates. Compared with ESWL, RIRS is associated with more rates of complication and longer stay in hospital (Geavlete et al., 2006; Lamb et al., 2011).

Many of the symptoms which increase the rates of complications are associated with the ureteral stents that is placed after the procedure. These polyurethane stent tubes are designed with distal and proximal coils to stay at their positions between the bladder and kidney. In spite of stents' advantages, the distal bladder coils might be felt by the patient and caused irritative voiding symptoms and haematuria (Pearle et al., 2005)

Table 2.2 Treatment algorithm of renal stones

Renal Stones (all locations except lower pole stone in size of 10-20 mm)		
> 20 mm	→	1. PCNL 2. RIRS or ESWL
10-20 mm	→	Endourology or ESWL
<10 mm	→	1. ESWL or RIRS 2. PCNL

Table 2.3 Treatment algorithm of lower-pole renal stones

The lower pole Stones (>20 mm & <10 mm)				
10-20 mm	→	Unfavorable factors for ESWL	→ YES	1. Endourology 2. ESWL
			→ NO	ESWL or Endourology

2.3.5 Percutaneous Nephrolithotomy (PCNL)

Percutaneous nephrolithotomies are mainly performed for stones greater than 20 mm in size (Figure 2.6). Different endoscopes, rigid and flexible, are suitable and the selection depends on the surgeon experience. Standard access tracts are 24 to 30F. Smaller access sheath which is thinner than 18 F, miniPCNL, were primary introduced for pediatrics but currently also in use for adults (Khan et al., 2016). For PCNL, the efficacy of miniaturized systems seems to be greater than standard PCNL, but the benefit on stone-free-rate has not been demonstrated yet. The miniPCNL can be associated with less loss of blood, but the operation time is longer (Ruhayel et al., 2017).

Laser, pneumatic and ultrasonic systems are mostly used for rigid nephroscopy (Ruhayel et al., 2017). Before the operation, ultrasonography or computed tomography support the identification of the tissue between the kidney and skin, then calyceal puncture is operated. This technique reduces the incidence risk of bowel and visceral injury (El-Shaer et al., 2019; Turk et al., 2016; Zhu et al., 2017). After access into the kidney is succeeded, a guidewire is inserted to the bladder antegrade for maintaining passage of balloon dilators or single dilator to expand the tract (Osman et al., 2005). When dilation and placement of the working sheath is done, both flexible and rigid nephroscopes might be passed for lithotripsy (Akman et al., 2011).

The contraindications of PCNL are untreated urinary tract infections, pregnancy and kidney tumors (Violette et al., 2016). The patient with a stone greater than 20 mm or staghorn calculi; percutaneous nephrolithotomy is the standard while decreasing the length of hospital stay by 75% in compare of open surgery (Preminger et al., 1985). PCNL is preferred as more efficient than RIRS or ESWL for many kinds of stones. However, the procedure is more invasive (Turk et al., 2016).

During the operation, irrigation pressure should be under 30 mmHg for preventing postoperative sepsis and other complications (Wu et al., 2017). Most commonly seen postoperative complications are urinary leakage, fever, bleeding and presence of residual stones (Turk et al., 2016).

2.4 Intrarenal Pressure during Endourology

According to international guidelines, the flexible ureteroscopes (f-URS) are the primary treatment option of kidney stones up to 20 mm (Assimos et al., 2016) (Pradere et al., 2018). To achieve better visibility during procedures, irrigation maintains clear image inside the urinary tract, while transporting the emerging stone dust and fragments. This irrigation relates with parameters of the irrigation inflow and outflow.

The irrigation inflow relates with the irrigation pressure set. In addition, it depends on the sizes of the working channel diameter for instruments. On the other hand, the irrigation outflow depends on the usage of a UAS and the size of the f-URS.

High level of intrarenal pressure might be reached in case inflow and outflow are not in equilibrium. The increase in the intrarenal pressure can trigger pyelovenous reflux and therefore the bacteria or other endotoxins in the collecting system may be transferred to the systemic blood flow. This may result in bacteremia and septic complications which might lead to prolonged antibiotic therapy, intensive care unit admission and even death. To prevent the mentioned complications, the intrarenal pressure should be kept below 40 cmH_2O.

In the study of Doizi et al. (2021), continuous monitoring of IRP during f-URS with use of a sensor wire is performed. Intrapelvic pressure is recorded at different conditions: Baseline pressure (a); pressure when scope is inserted with stable irrigation flow with the irrigation pressure calibrated at 80 cmH_2O (b); the pressure when manual irrigation ceased in small brisk movement (c); the pressure when manual irrigation applied continuous and gradually (d); the pressure during lithotripsy (e) (Doizi et al., 2021).

They employed the 0.014″ PressureWireX guidewire (St. Jude Medical, USA) that have indication for cardiology as assessing fractional flow reserve (FFR) procedures in coronary arteries. PressureWireX guidewire have a digital sensor located at 3 cm proximal of the wire end for measuring the pressure. The soft platinum and distal 3 cm part are floppy, radiopaque and hydrophilic that allows minimal trauma during positioning. The polytetrafluoroethylene coated main shaft, the last 28 cm part, is hydrophilic and flexible.

The console, QUANTIEN system, receives the pressure signal wirelessly from the wire. The screen of QUANTIEN system can display the pressure and temperature values. The pressure values are displayed in mmHg, at the range from -30-300 mmHg which is -40.8 to 407.9 cmH_2O (Doizi et al., 2021).

After placement of the pressure sensor guidewire, IRP measurements were obtained in five cases. The average baseline of intrarenal pressure (a) was 6 cmH_2O. During flexible URS and irrigation pressure was at 80 cmH_2O, without forced irrigation, the average intrarenal pressure (b) was 63 cmH_2O. Mean intrarenal pressure during laser lithotripsy (e) with on demand forced irrigation was 115.3 cmH_2O. The highest pressures recorded during lithotripsy ranged from 289.3 to 436.9 cmH_2O (Doizi et al., 2021).

The maximum-minimum, mean, peak pressure values, pressure patterns with and without the f-URS and the effect of on demand irrigations were examined in the study of Doizi et al. (2021). However, the pressure peaks only observed and reported for short durations. The longest duration of measurement, the study of Schwalb et al. (1993) on pigs, was shown that prolonged exposure which is longer than 45 min, the intrarenal pressure is exceeded 200 cmH_2O. The high-pressure value was associated with inflammation and renal scarring.

In literature, there is no evaluation of irrigation methods such as gravity-based or automatic irrigation systems. Thus, no irrigation method is recommended as the best option.

3. MATERIALS AND METHODS

3.1 Materials

3.1.1 Pressure sensor

PressureWire™ X Guidewire is a catheter inserted through a blood vessel for measuring the physiological parameters in the cardiac and peripheral blood vessels by cardiologists. The PressureWire™ X Guidewire can measure blood pressure and blood temperature via integrated sensor element at the tip. The cardiologists use PressureWire™ X Guidewire to assess Fractional Flow Reserve (FFR) in coronary vessels in Cath Lab (Figure 3.1).

Figure 3.1 The system integration of PressureWire™ X Guidewire system in Cath Lab

In this thesis study, the pressure sensor and console that called QUANTIEN system, was used as intrarenal pressure monitoring device. The sensor wire has diameter of 0.014″, 1Fr. The digital sensor is placed at the 3 cm distal of the wire and this area is made of soft floppy, hydrophilic and radiopaque platinum. Proximal polytetrafluoroethylene coated side of the wire is flexible and hydrophilic (Figure 3.2).

The signal of pressure is transmitted wirelessly to QUANTIEN system where the pressure and temperature can be displayed simultaneously. The pressure is measured in range from -30 to 300 mmHg. All pressure values in cmH2O is converted by multiplying value in mmHg by 1,35. The accuracy of sensor wire is ≤ 2mmHg or ± 2%. Fortunately, sensor is digital and can be calibrated quickly.

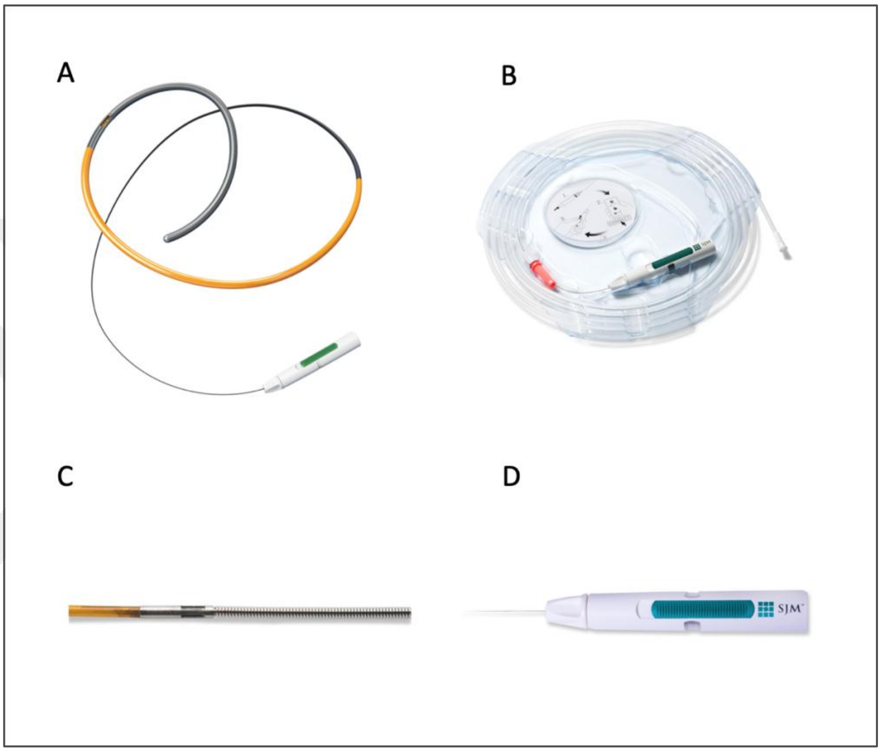

Figure 3.2 The PressureWire™ X Guidewire (A), packaging coil (B), sensor element close-up view (C) and wireless transmitter (D)

3.1.2 Imaging System

Imaging system was used for visualizing the cavities where the pressure values were measured. The cavities were 3D printed kidney model, sheep and patient kidney. During 3D model and sheep kidney experiments, URF-P5 (Olympus, Japan) and Flex-X2S (Karl Storz, Germany) were used. These flexible fiberscopes were connected to laparoscopic camera head which was inserted to Olympus and Storz video processors (Figure 3.3).

Figure 3.3 The imaging system

3.1.3 Flexible Ureteroscope

The URF-P5 flexible fiber ureteroscope (Olympus, Japan) was used access to the kidney in endourologic operation and in-vitro experiments. The scope is designed to pass the ureter; examine the entire kidney with 275° of down angulation and 180° of up angulation. The tip of scope is 5.3 Fr and the working channel is 3.6 Fr. The length of the scope is 1050 mm; working length is 700 mm.

3.1.4 Percutaneous Nephroscope

The 16.5/17.5 Fr PCNL Sheath, Optimum PNL (MIG Optimal Medical, Turkey) was used during PCNL in operating room. The 12Fr nephroscope (Karl Storz, Tuttlingen, Germany) was inserted into the PCNL sheath and connected to imaging system.

3.1.5 Flushing Pump

Obtaining certain flow rate during in-vitro test with sheep kidneys and 3D printed model, the flushing pump OFP-2 (Olympus, Japan) was used. The pump was for gastroenterological procedures to clean the gastrointestinal tract with sterile water for clearer image during the endoscopies.

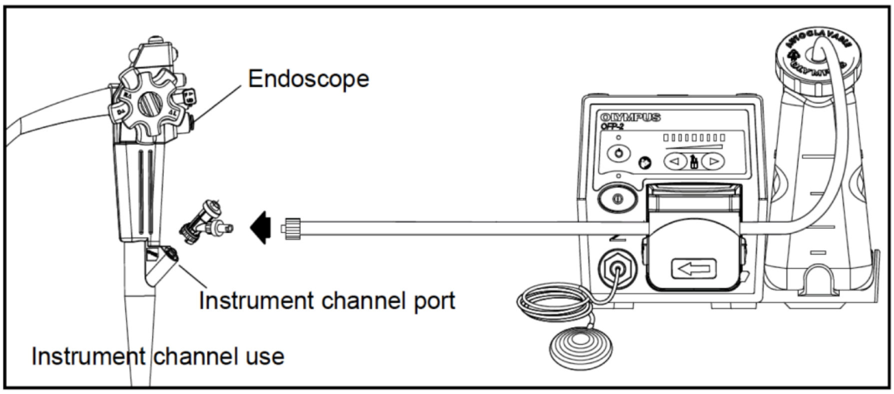

Figure 3. 4 The connection of scope and flushing pump

The pump was connected to scope, URF-P5, through the working channel (Figure 3.4). The reusable tubing set was used, the container was filled with saline. The flushing pump was connected to scope then scope was connected to camera head of imaging system (Figure 3.5). The device had 9 levels of flow rate, each level can be seen on front panel. Due to probability of loosening on tubing set, the flow rates were measured manually. The flow rates of each level are given in Table 3.1.

Figure 3.5 The flushing pump was connected to URF-P5 through the working channel and f-URS was connected to camera head of imaging system

Table 3.1 The flow rates of each levels on OFP-2 Flushing Pump

LEVEL	FLOW RATE (ml/min)
Level 1	135
Level 2	150
Level 3	210
Level 4	240
Level 5	300
Level 6	360
Level 7	420
Level 8	420
Level 9	420

3.1.6 Fluid Pump

A medical fluid pump (Vimex Endoscopy, Poland) designed to deliver fluid under a given pressure to an operative field (Figure 3.6). The device provides working modes of arthroscopic, hysteroscopic and urologic surgeries. The pump was connected to scope, URF-P5, through the working channel. The reusable tubing set was used, the saline was hung. The device has adjustment for pressure in mmHg and flow in l/min; in range between 10-150 mmHg and 0,1-1,0 l/min, respectively.

Figure 3.6 The fluid pump with saline connection

3.1.7 Designed Ureteral Access Sheath (UAS)

Olympus ureteral access sheath, UROPASS (Olympus, Japan) was used during in-vitro tests. The size of UAS was 10/12Fr. and 54cm in length. The UAS was assembled together with 4Fr. ureteral catheter (Cook Medical, USA). Ureteral catheter was used as pressure sensor channel during experiments (Figure 3.7).

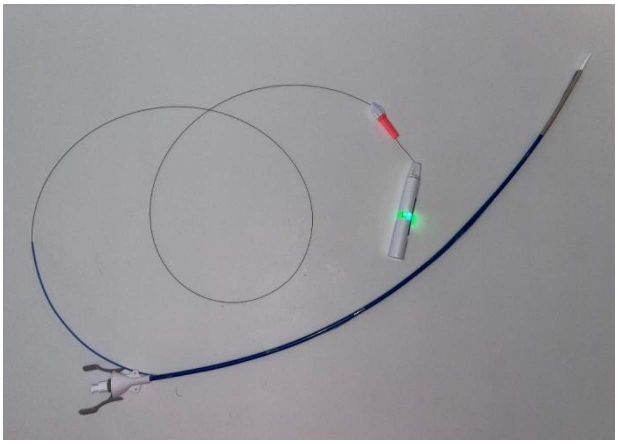

Figure 3.7 Designed ureteral access sheath with pressure sensor guidewire

3.1.8 Designed Ureteral Catheter

Ureteral catheter, Dual Lumen Ureteral Access Catheter, 10 Fr, (Cook, Bloomington, Ca) was used during endourological procedure, PCNL. The catheter has two port; one for balloon insufflation and second for pressure sensor, PressureWire™ X Guidewire (Figure 3.8).

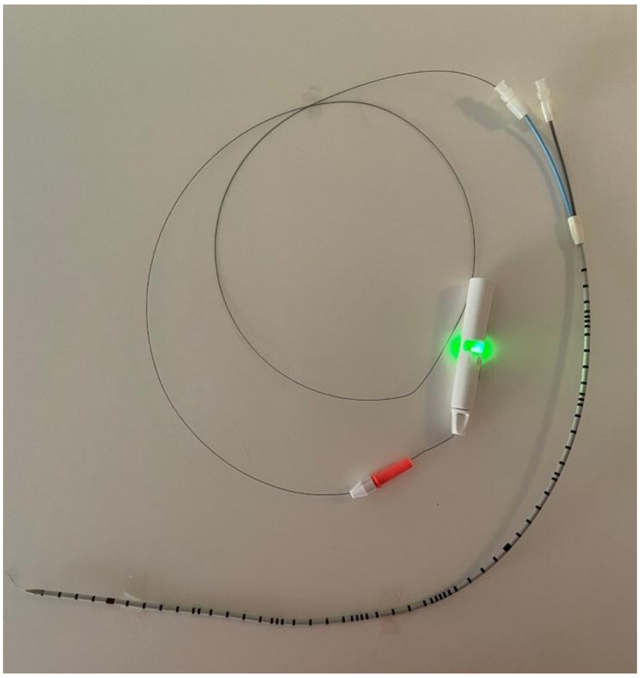

Figure 3.8 Designed ureteral access sheath with pressure sensor guidewire

3.1.9 Animal Kidneys

6 sheep kidneys were used for in-vitro tests with designed UAS. The sizes of the kidneys were shown in Table 3.2.

Table 3.2 The Wide (W), length (L) and height (H) of the sheep kidneys

Model	**Kidney size (cm)**		
	W	L	H
1	5.60	3.30	1.70
2	5.50	3.30	2.10
3	5.30	3.00	2.00
4	5.30	3.10	2.10
5	4.80	2.90	1.70
6	4.50	2.90	1.60

3.1.10 3D Printed Kidney Model

The 3D printed kidney model was used for primary tests to get an initial measurement from pressure sensor. The 3D mechanical drawing of the model for f-URS was illustrated in Figure 3.10-11. The ureter and kidney were printed in 8 hours. The 3D printer was constructed piece by piece so that brand name cannot be given (Figure 3.9). The PLA was used for printing and pieces were resembled with hot glue gun. Leakage for liquid was tested after resemble process.

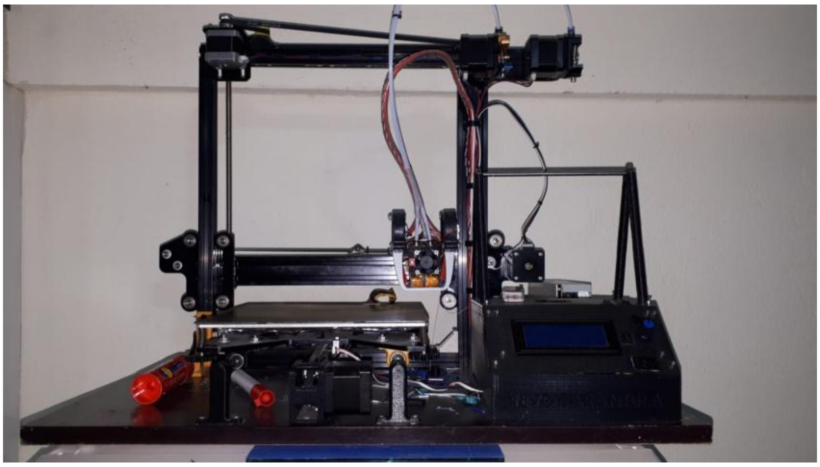

Figure 3. 9 3D Printer

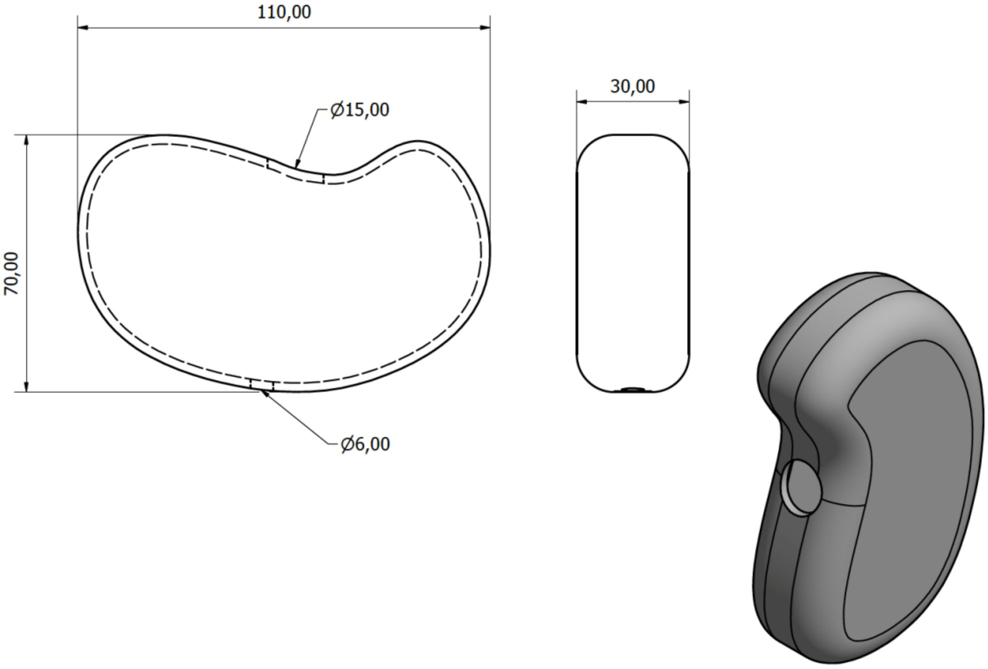

Figure 3. 10 The mechanical drawing of kidney for 3D Printer

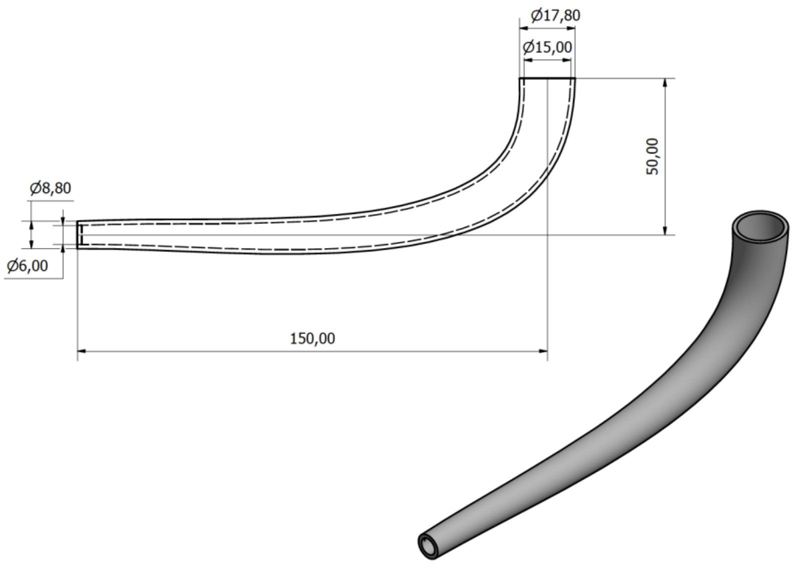

Figure 3.11 The mechanical drawing of ureter for 3D Printer

3.2 Methods

3.2.1 Pressure Monitoring in 3D Printed Model with UAS

The 3D printed kidney model was obtained from 3D printer for primary tests to examine the pressure sensor accuracy. The PressureWire X guidewire was opened as sterile package and used during tests in operation room. The sensor guidewire was calibrated after the sensor inserted through the ureteral access sheath inside the 100ml syringe (Figure 3.12).

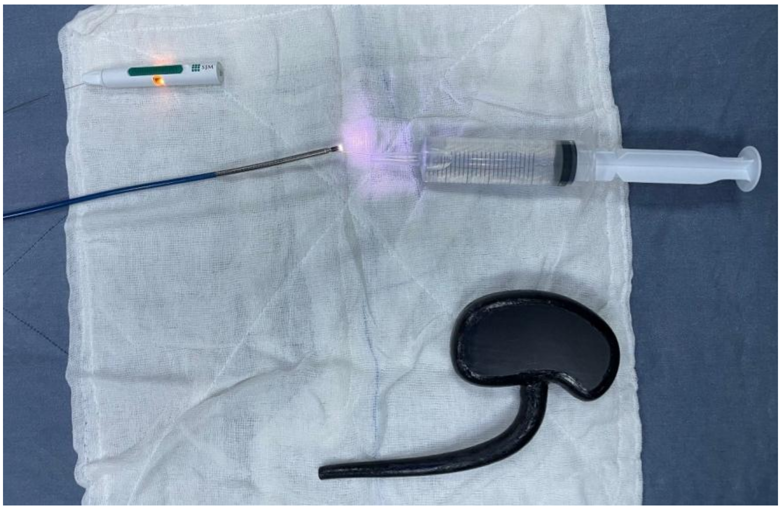

Figure 3.12 Sensor guidewire calibration

The UAS was inserted into the 3D kidney model then the ureteroscope, URF-P5 was driven inside the sheath. During the 3D model test due to stiffness of the PLA, ureter cannot be expanded so that there was limited diameter. The catheter could not be used for sensor coverage, so that the sensor inserted through the UAS. The URF-P5 was attached to camera head of imaging system (Figure 3.13). The position of the sensor was confirmed simultaneously along the measurements (Figure 3.14).

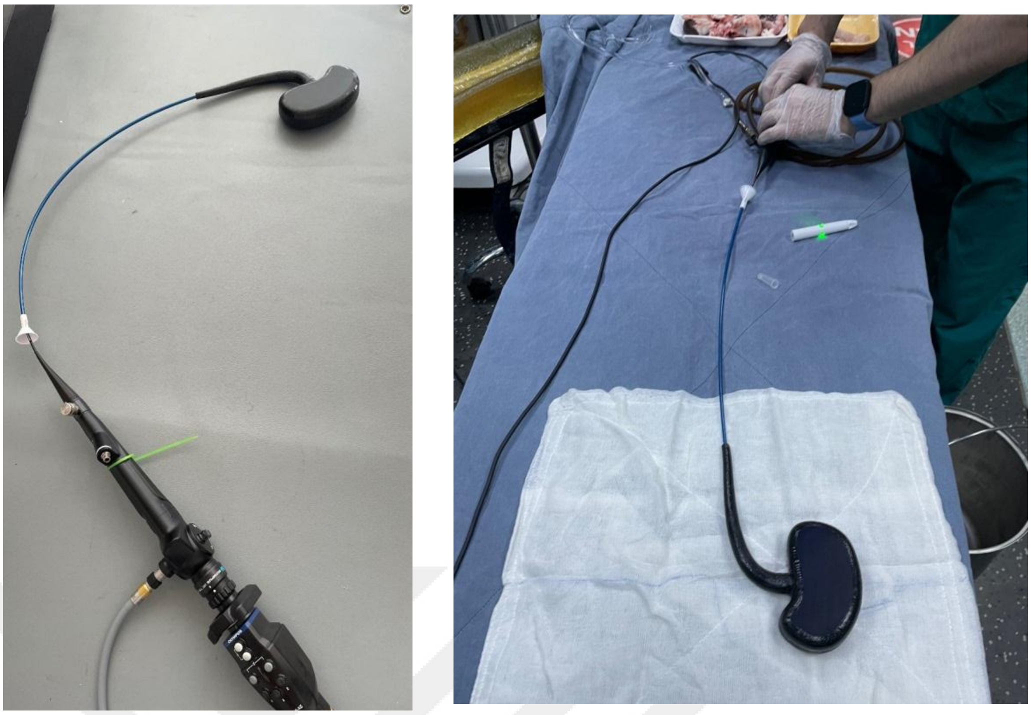

Figure 3.13 The 3D printed model with UAS test setup

Figure 3.14 The image of the pressure sensor inside the UAS

In the other experiment on 3D printed model, the fluid pump (Vimex Endoscopy, Poland) was utilized. The UAS was inserted into the 3D kidney model then the ureteroscope, URF-P5 was driven inside the sheath, next to sensor guidewire (Figure 3.15). The fluid was adjusted to 0.20 l/min. The pressure value was increased from 10 to 30 mmHg; 3 different pressure value was examined (Figure 3.16).

Figure 3.15 The fluid pump experiment setup

Figure 3.16 The fluid pump pressure adjustment

3.2.2 Pressure Monitoring in Animal Kidney with UAS

The imaging system Evis Exera III (Olympus, Japan) and the ureteroscope, URF-P5 (Olympus, Japan) were used as imaging systems during the tests. The QUANTIEN system was placed on the imaging tower. The flushing pump OFP-2 was connected to URF-P5 through the working channel with reusable tubing set, the green lid container of the pump was filled with saline (Figure 3.17). The PressureWire X guidewire was opened as sterile package and used during tests in laboratory. The sensor guidewire was calibrated after the sensor inserted through the ureteral access sheath inside the 100ml syringe.

The UAS was inserted into the 6 sheep kidney model then the ureteroscope, URF-P5 was driven inside the sheath. The sizes of sheep kidney is given in Table 3.2. The size of animal kidney and the ureter diameters were thinner than human kidney. As a result, the 10/12Fr with catheter was extensive. The pressure sensor was inserted through the UAS.

Figure 3.17 The setup of the experiment

The 6 sheep kidney’s ureter was dilated with dilator of the UAS. The 54 cm UAS was placed after dilation process, the ureteroscope and sensor guidewire inserted meanwhile. Avoiding the separation of UAS and ureter with irrigation pressure, the distal of the ureter was knotted by suture (Figure 3.18). The position of the sensor was confirmed simultaneously along the measurements (Figure 3.19).

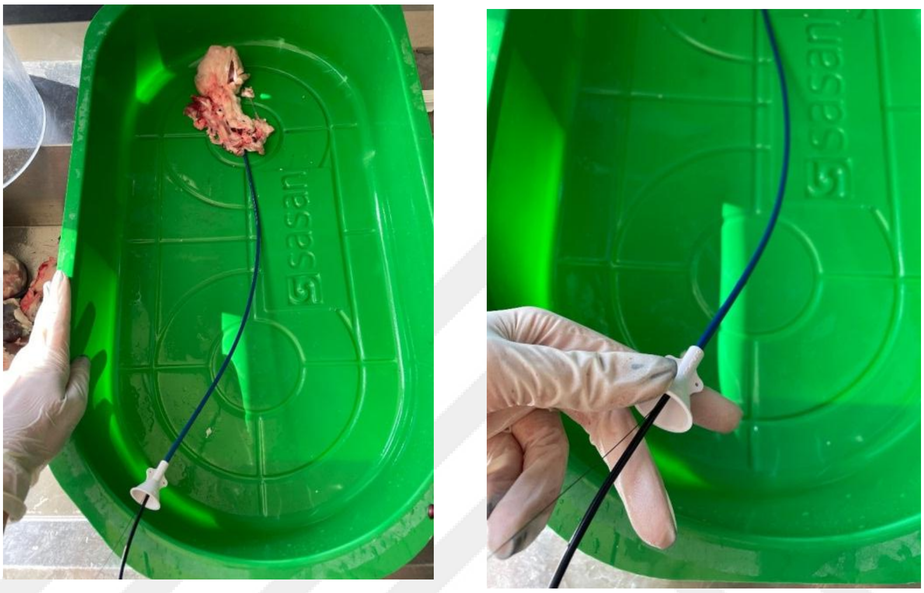

Figure 3.18 The placement of UAS and animal kidney

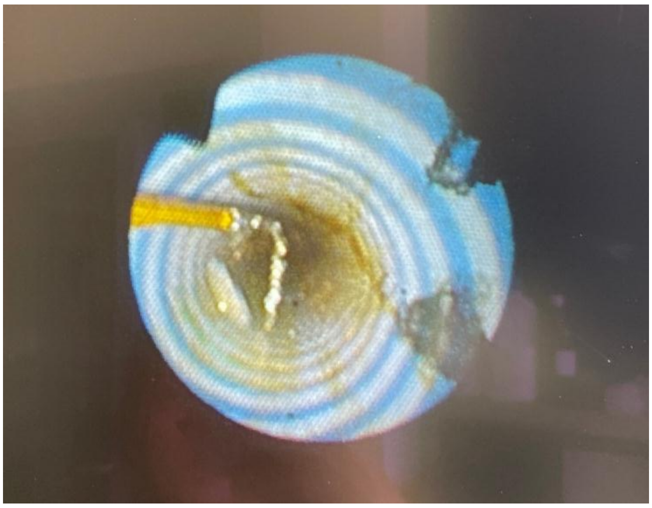

Figure 3.19 The location of sensor through the UA

3.2.3 Pressure Monitoring During PCNL with Ureteral Catheter

The operation was performed by Assoc. Prof. Dr. Mehmet Ilker GOKCE, MD in Ankara University Ibn-i Sina Hospital, Department of Urology. The male patient was under general anesthesia. The stone burden can be seen in the C-arm fluoroscopy monitor. The calyx structure can also be seen on the image, the darker spot was the kidney stone (Figure 3.20).

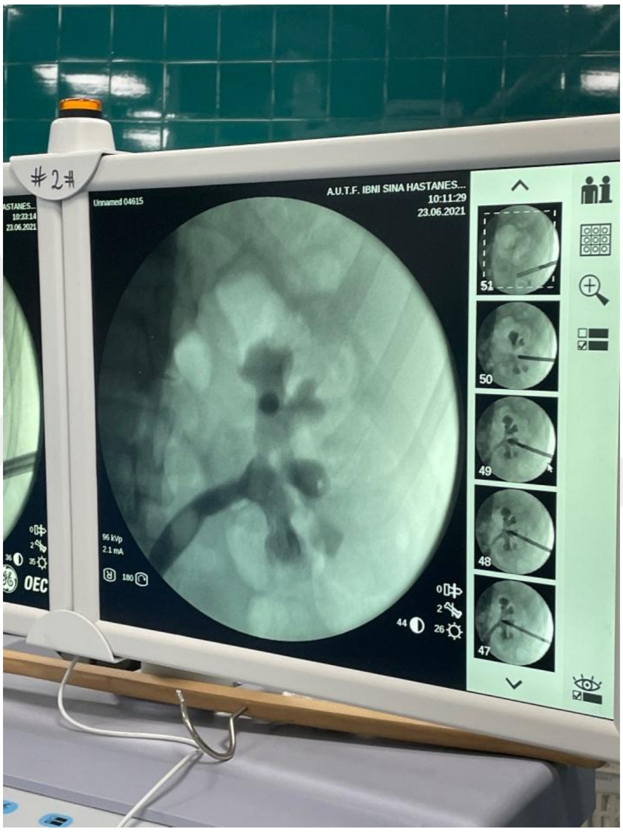

Figure 3.20 C-arm fluoroscopy monitor

The ureteral catheter was inserted retrograde to urinary tract to perform retrograde pyelography during Percutaneous Nephrolithotomy (PCNL). Renal access was performed under fluoroscopy guidance and tract was dilated with a metallic dilator to 16 Fr and a 17 Fr metallic sheath (MIG Optimal medikal, Ankara, Turkey) was inserted over the dilator. A 12 Fr nephroscope was used to access the kidney. The percutaneous access and operation layout were given in Figure 3.21.

Figure 3.21 The percutaneous access and operation layout

The kidney stones were fragmented by Ho:YAG laser (Dornier Medilas H Solvo 35, Germany). The pressure measurements were started after the stone lithotripsy. The measurements were taken from emptied renal cavity. The sterile package PressureWire X guidewire was opened on sterile desk (Figure 3.22). Firstly, the sensor was calibrated, syringe with saline was attached to distal end of guidewire’s packaging coil. After the saline was filled into the packaging coil through the flushing port, the transmitter was turned on (Figure 3.23). The system was zeroed and guidewire was removed from packaging coil.

Figure 3.22 The package of PressureWire X guidewire.

Figure 3.23 Zeroing the guidewire

The first measurement was performed from the renal pelvis, while the ureteral catheter with sensor was placed through the ureter with the tip of the pressor sensor was located in the renal pelvis. The sensor placement was simultaneously controlled by nephroscope image, also the sheath location was controlled at intervals by fluoroscopy (Figure 3.24). The irrigation was attached to inflow valve of nephroscope sheath. The pressure measurement was taken in two different way: the nephroscope sheath is closer and far away from nephroscope (Figure 3.25). So, the outflow of the system was changed. In the location of sheath was pulled back from nephroscope (Figure 3.25a), due the outflow was supplied from the valves on the sheath, there was reduction of outflow. The active aspiration was also activated, the changes on the pressure were monitored.

The second measurement was taken when the f-URS was inserted antegrade from PCNL sheath. The irrigation was sustained from working channel of f-URS. With and without aspiration, the pressure values were monitored.

Figure 3.24 The simultaneous image of sensor guidewire

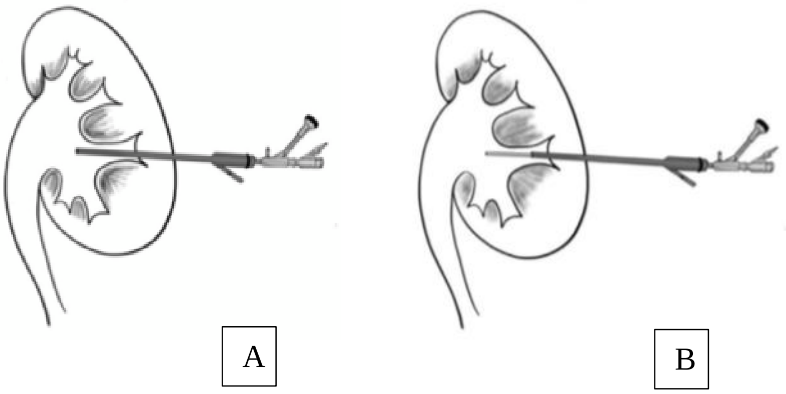

Figure 3.25 The locations of nephroscope and sheath (Gokce et al., 2021)

4. RESULTS

To obtain accurate results of pressure sensor guidewire with designed ureteral access sheath and ureteral catheter, experiments were performed in 3 different setups. The primary experiments were performed with UAS in 3D printed kidney model which produced as approximate to human kidney sizes. Second experiment was on animal kidney. The sheep kidney was used to test UAS in narrow renal cavity. The last but most important experiment was performed on human kidney during endourological procedure, percutaneous nephrolithotomy. The performance of pressure sensor guidewire within the ureteral catheter was examined.

4.1 Pressure Measurement in 3D Printed Model with Designed UAS

In the first experiment on 3D printed model, the fluid pump (Vimex Endoscopy, Poland) was utilized. The setup was given in Figure 3.15. The pressure value was increased from 10 to 30 mmHg while the fluid flow was set to 0.20 l/min. The pressure results were given in Table 4.1. This experiment was performed to confirm the sensor guidewire accuracy.

Table 4.1 The pressure values of 3D printed model with fluid pump

Fluid Pump Flow (l/min)	Fluid Pump Pressure (mmHg)	Pressure Sensor (mmHg)	Pressure Sensor (cmH_2O)
0.2	10	9	12,15
0.2	20	21	28,35
0.2	30	29	39,15

The second experiment setup was given in Figure 3.13, in Section 3.2.1. The results were captured from QUANTIEN monitor with USB. In the data screen, “Pd” value was the instant pressure value that acquired from the sensor element (given at Figure 4.2). “Pa” values only had importance during FFR procedure, in cardiology. In “FFR” segments of the QUANTIEN screen were shown the calculation of “Pd/Pa”.

Table 4.2 The pressure values of 3D printed model with flushing pump

Flushing Pump Level	**Flow Rate (ml/min)**	**Pressure (mmHg)**	**Pressure (cmH_2O)**
Level 1	135	9	12,15
Level 2	150	18	24,3
Level 3	210	29	39,15
Level 4	240	37	49,95

The pressure values were taken after the model was filled with saline by using OFP-2, the flushing pump. First 4 level of pump was used, however the pump had 9 levels, the experiment was terminated when pressure was reached approximately 40 cmH_2O. The pressure value was the critical level to cause post-op complications. PressureWire X was calculated pressure in units of ‘mmHg’ so that all the test data were converted to cmH_2O by multiplying 1,35.

As expected, it was observed that the pressure measurements increased with the increase of the flushing pump’s flow rate (Figure 4.2). At the minimum flow rate, 135 ml/min, the pressure was measured as 12,15 cmH_2O. The flow rates at 150, 210 and 240 ml/min resulted in 24, 39 and 50 cm H_20 pressure, respectively (Table 4.2).

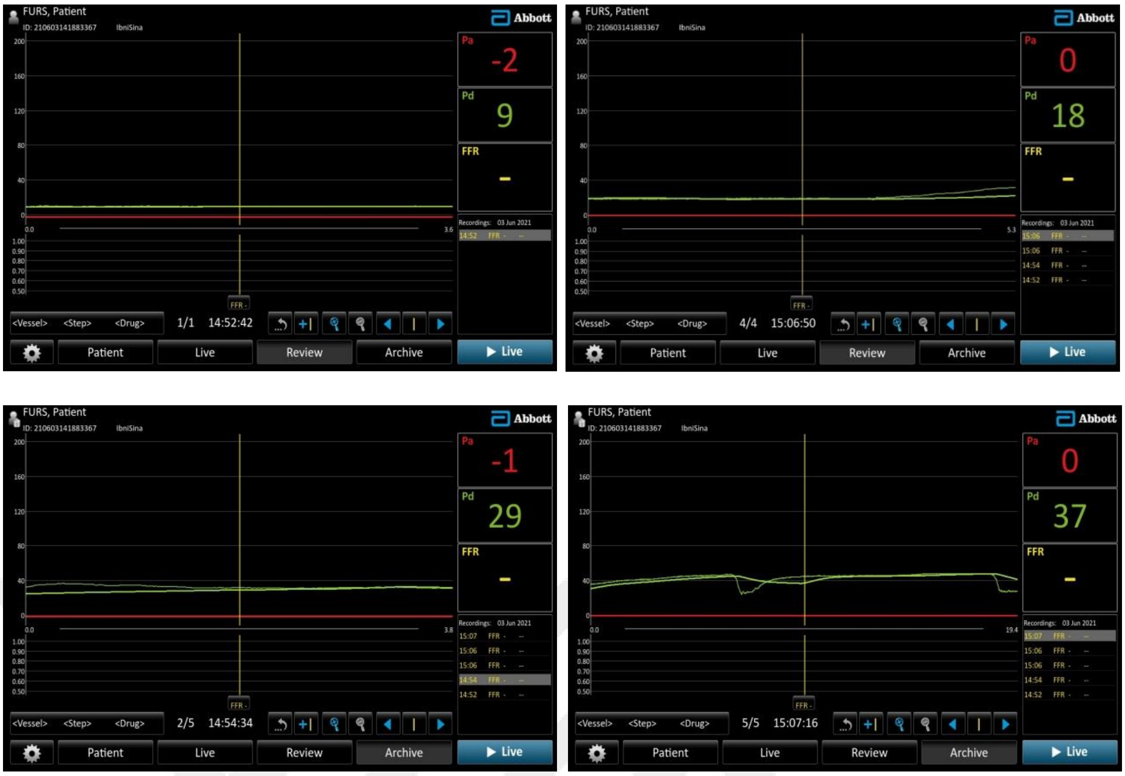

Figure 4.1 The pressure readings of 3D Printed Models

The graph of the results is given in Figure 4.2. As mentioned before, the experiment was terminated when the system pressure was reached to 40 cmH_2O. In the graph, critical level was indicated with red line, in Level 3 with 210 ml/min, almost the maximum pressure value was reached with automatic pump.

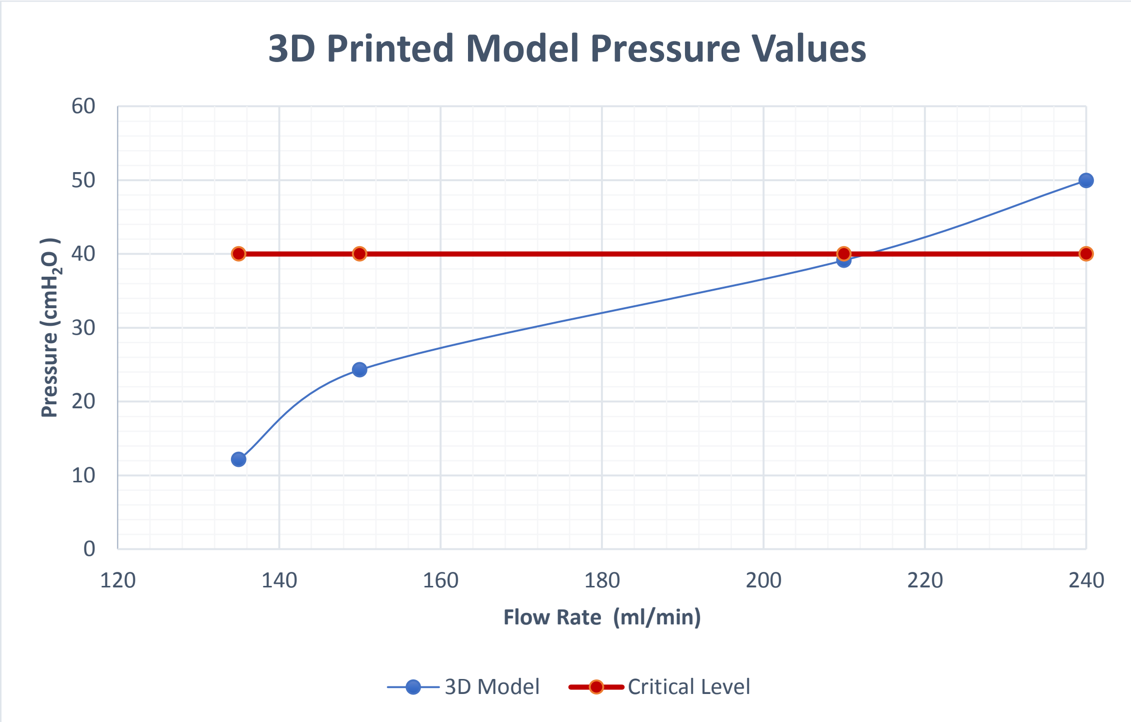

Figure 4.2 The graph of pressure values

4.2 Pressure Measurements in Animal Kidney with Designed UAS

The sizes of the sheep kidney were significantly smaller than human kidney. The mean weight, length and height dimensions were 517, 308 and 187 mm, respectively. As a result, the pressure in 6 sheep kidneys reached the critical value between the Level 2 to 3. The kidneys were filled with saline by flushing pump and the pressure readings were started, after the determined base pressure 4.0 mmHg was obtained. The pressure inside the renal cavity was increased by the increase of flow rate (Table 4.2).

Table 4.3 The pressure changes in animal kidneys

Model	Kidney size (mm)			Pressure (cmH_2O)			
	W	L	H	Base	Level 1	Level 2	Level 3
				-	135 ml/min	150 ml/min	210 ml/min
1	560	330	170	5,4	9,45	28,35	109,35
2	550	330	210	5,4	20,25	39,15	83,7
3	530	300	200	5,4	24,3	37,8	83,7
4	530	310	210	5,4	8,1	32,4	91,8
5	480	290	170	5,4	17,55	37,8	89,1
6	450	290	160	5,4	10,8	27	76,95

The pressure readings were recorded in 20 second in each level. The QUANTIEN system were calculated the average pressure value in that 20 seconds and displayed. The displayed images given in Figure 4.3 were obtained at level 2 with 150 ml/min flow rate. The mean pressure was 33,75 ± 4.80 cmH_2O. The whole pressure data and critical level of IRP is given in Figure 4.4.

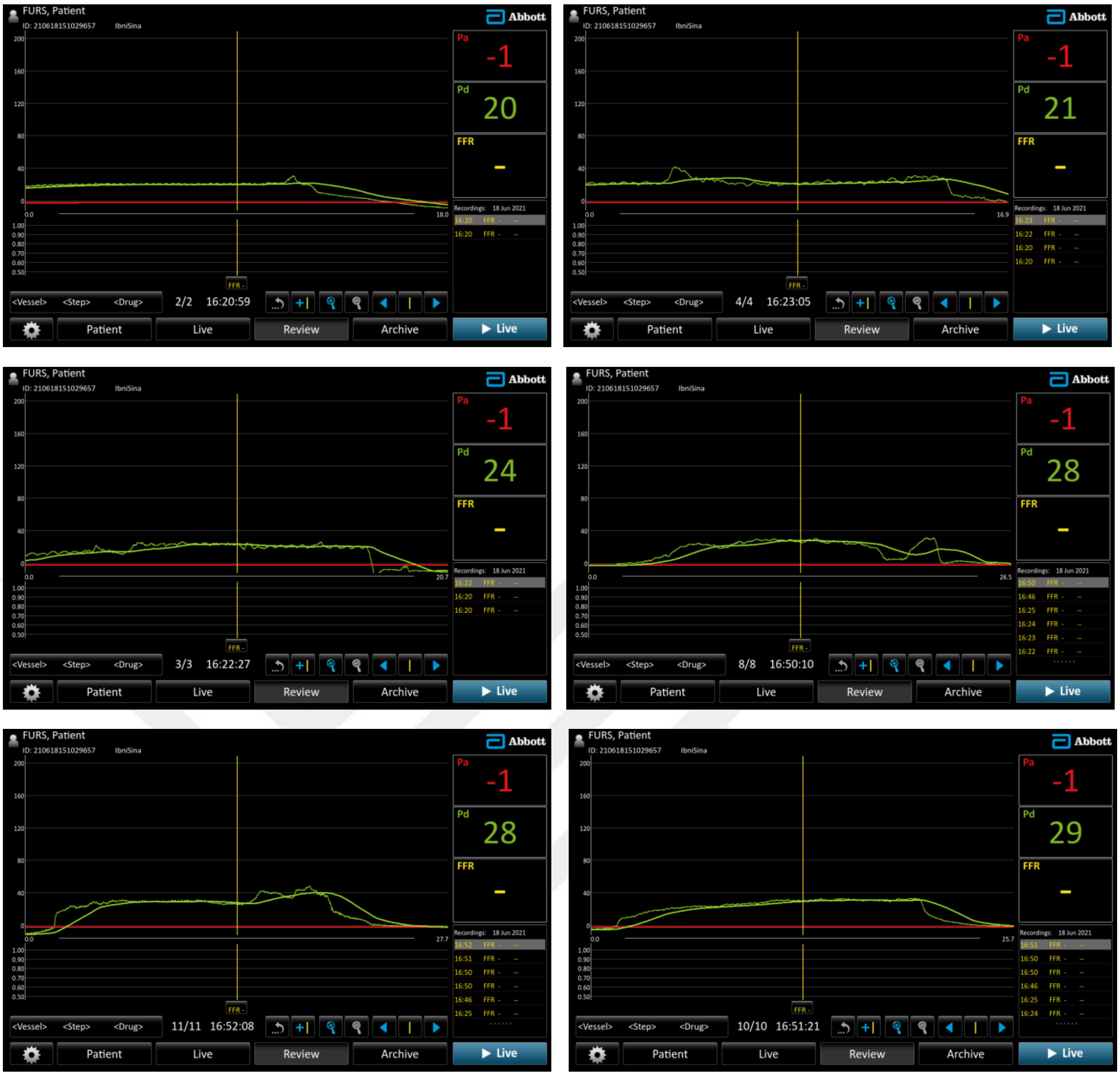

Figure 4.3 The pressure readings of animal models in Level 2

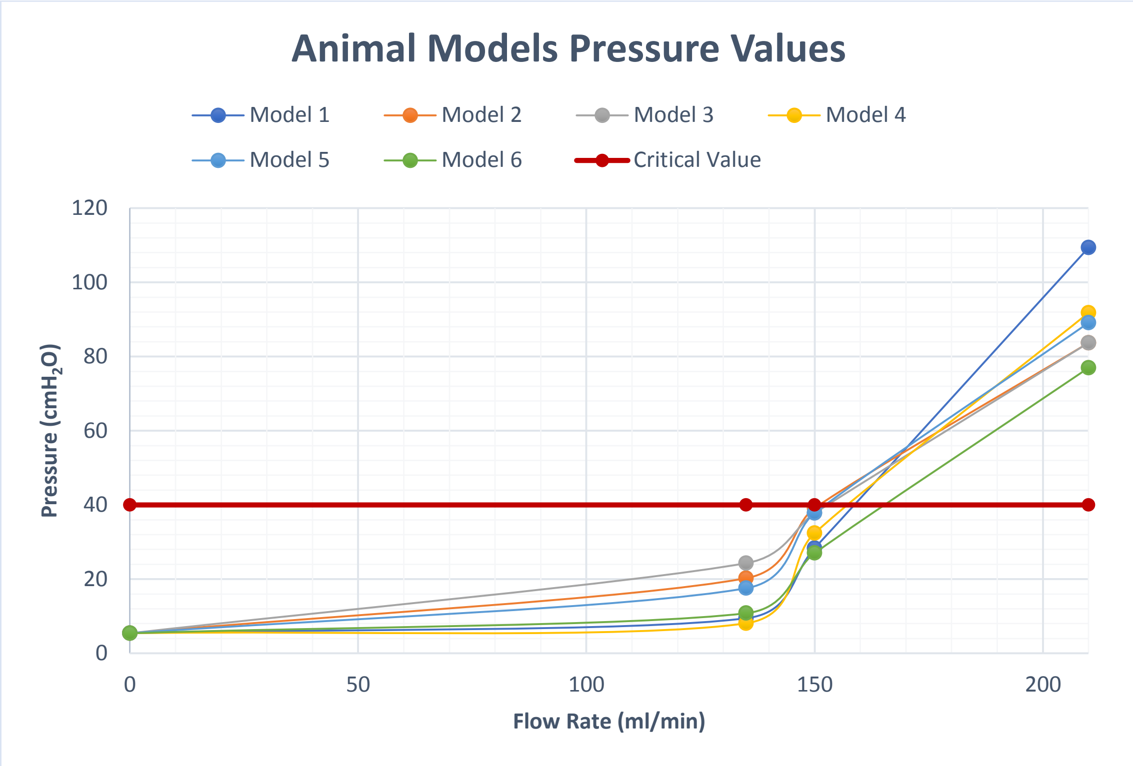

Figure 4.4 The graph of pressure values in animal models

4.3 Pressure Results During PCNL with Designed Ureteral Catheter

The final experiment was on the human kidney, during endourology. The pressure readings were started after the stone free status was established by Dr. Gokce. Pressure measurements in 2 different procedures and settings were mentioned in Section 3.2.3 in detail.

First pressure measurements were obtained in 4 different time intervals (Figure 4.5). Time interval "1" was the base pressure when nephroscope and sheath were in the same positon and pressure guidewire was inserted from ureteral catheter. Adding to this, gravity irrigation was used.

The renal base IRP was measured as 5,4 cm H_2O. After the manual irrigation was executed, the pressure was increased to maximum of 12,15 cm H_20 as showed in time interval "2". The third time interval is the replacement of nephroscope and sheath.

During the measurement, the sheath which sustained the outflow of the irrigation was pulled back from nephroscope, the pressure was increased approximately to 30 cm H_20. In that point, without reaching to critical level, the active aspiration was supplied. With the active aspiration, the decrease of the pressure was achieved. Unfortunately, the sensor element was collapsed within the renal collecting system due to aspiration and caused increase in the pressure (Figure 4.6). The aspiration was paused, the sensor relocated within the cavity and the measurements were continued. With the aspiration, the instant IRP was lowered in time interval “4”.

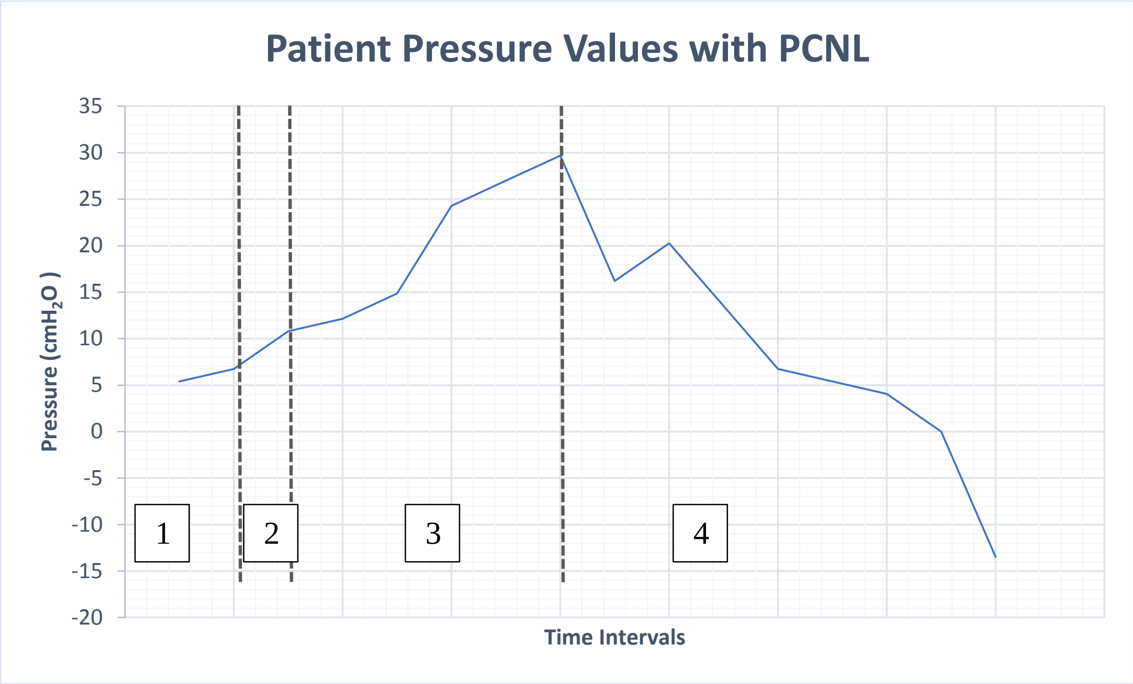

Figure 4.5 The graph of patient pressure values during different time intervals in PCNL

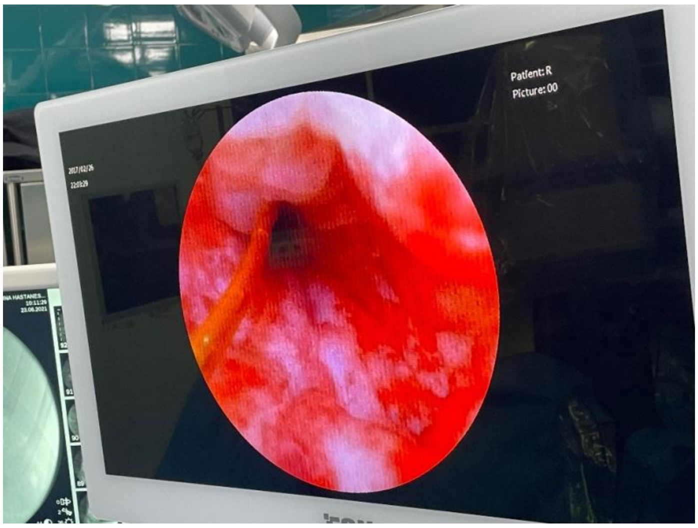

Figure 4.6 The collapse of the sensor within the renal collecting system

In the second procedure, the 5.3 Fr. ureterenoscope was inserted antegradely from nephroscope sheath (Figure 4.7). The gravity-based irrigation inflow was supplied from 3.6 Fr working channel of ureterenoscope. The base IRP pressure was 10 cmH_2O, approximately (Figure 4.7-1). When the irrigation increased manually, the pressure was reached to 16 cmH_2O (Figure 4.7-2). Due to thinness of working channel, the pressure increase was limited compared to nephroscope irrigation inflow capacity. After the active aspiration was turned on, the pressure was decreased (Figure 4.7-3).

The QUANTIEN system was captured the pressure measurement as a graph at the end of the examination. The complete pressure values in chart format and graph can be sustained from the system. As shown in Figure 4.8, after neglecting the peak values originated during the insertion and relocation of sensor guidewire, the critical level of 40 cmH_2O was tried not to exceed.

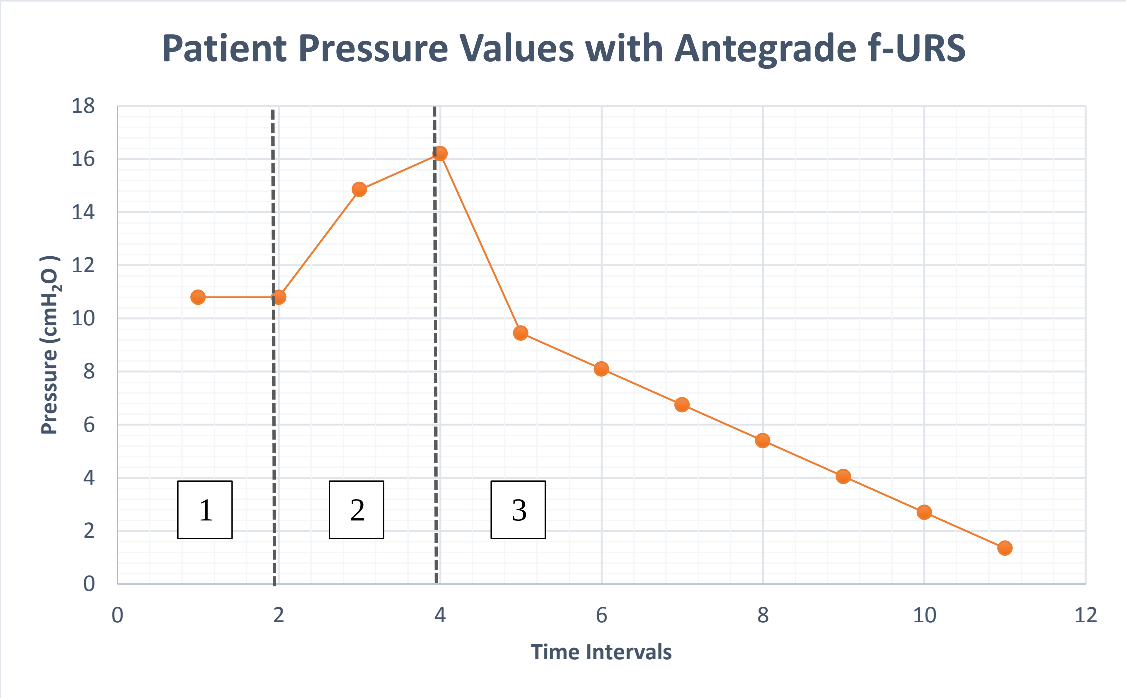

Figure 4.7 The graph of patient pressure values in antegrade f-URS insertion

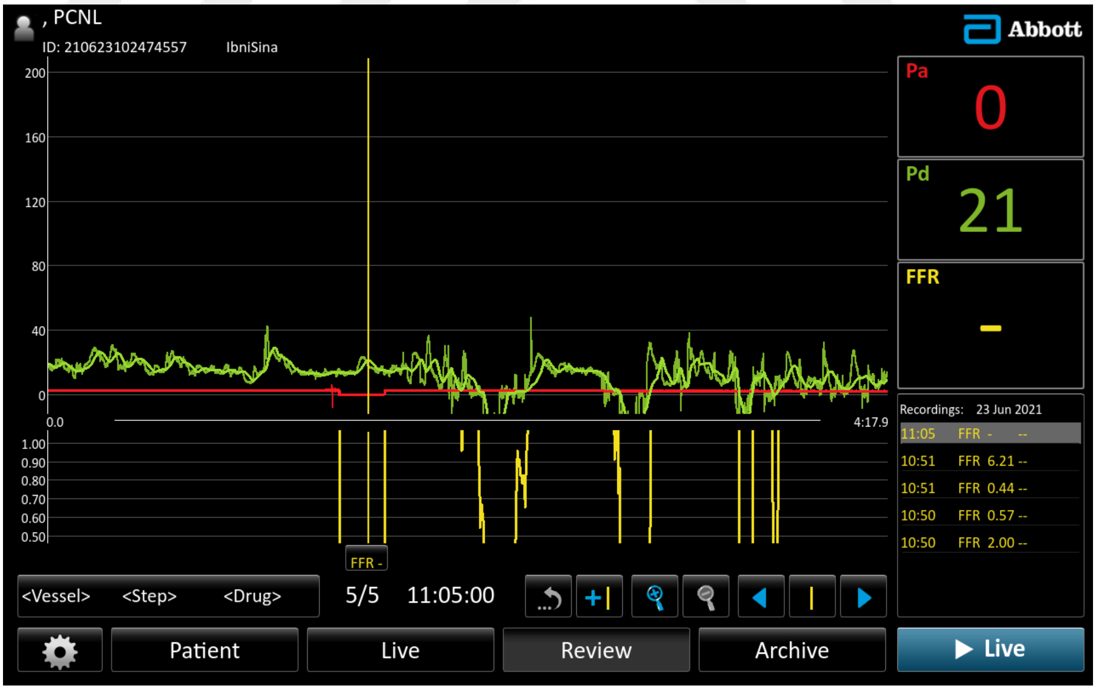

Figure 4.8 The overall graph of the pressure readings during PCNL

5. DISCUSSION AND CONCLUSION

5.1 Discussion

This thesis study aimed to generate a real time pressure monitoring during endourological process. For this reason, a ureteral catheter for percutaneous nephrolithotomies and ureteral access sheath for retrograde intrarenal surgeries was implemented. The pressure sensor guidewire, which was mainly in use for cardiology, was utilized as digital sensor element that monitoring the pressure inside the intrarenal cavity. A 3D printed model, animal kidney and patient were the 3 different experiment setups for examining the endourology disposables with sensor.

Endourological procedures aim to clear stones without causing post-op complications (Gokce et al., 2021). The main aim of researches and biomedical applications in endourological procedures were the improvement of the image quality by achieving better irrigation flow and irrigation pressures (Tokas, Herrmann, et al., 2019). During procedures, there are possible ways to maintain lower pressure values even working with high irrigation flow (Alsmadi et al., 2018; Rawandale-Patil et al., 2019). During the procedures, the intrarenal pressures should be under control, below the 40 cmH_2O or 30 mmHg should be maintained to avoid post-op complications (Monga et al., 2004). Unfortunately, an in-vivo human and ex-vivo animal experiment which pressure measurement on designed disposable with digital sensor cannot be found in literature. In this respect, the experiments and design of disposables might be significant. The studies in literature were performed to analyze the prolonged exposure of irrigation; cause of post-op renal scarring and inflammation; pressure in different locations of scopes; the pressures differences between baseline and lithotripsy; effect of PCNL sheath size on pressure.

In literature, all the experiments were performed by system of urodynamic pressure measurement except the study of Doizi (2021). In that study, they performed f-URS with PressureWire in 4 patients. The baseline pressure, pressure during therapeutic period were measured. In this thesis, the accuracy of the digital pressure sensor guidewire was first tested with a 3D printed model experiment in 2 different setups. The implemented sensor guidewire showed that the sensor can be utilized as real time pressure monitoring system.

Initial experiment on 3D model was with fluid pump in urology mode. With constant irrigation flow rate of 0.2 l/min, the pressure on system was set to vary from 10 to 30 mmHg. The real time pressure values on QUANTIEN monitor significantly showed that the relative error of the sensor at around 10 mmHg is around 10%. However, while the pressure increased to 20-30 mmHg, the relative error is around 5%. The pressure accuracy rate in the Abbott's Instruction for User Manual is ±2% for cardiological systems which is more isolated environment inside the arteries. The preferred pressure values in operations such as 20-30 mmHg have 5% of accuracy rate which is an acceptable result during endourology measurements due to leakages throughout the experimental setup. Second experiment's results given in Figure 4.2 showed that the pressure increases with the increase of the flushing pump flow rate. The flushing pump operating for gastroscopes, colonoscopes for cleaning the upper and lower gastrointestinal tract. The system had 9 level with increasing flow rate. The monitoring was terminated when the pressure reached to critical pressure value of 40 cmH_2O.

During 3D model experiments, due to the stiffness of the printing material, the PLA, the ureteral access sheath cannot be inserted with sensor catheter. So that the catheter was separated and the sensor was inserted next to the flexible scope, through the UAS. The reason of experiments was to test the accuracy of the sensor. The model was printed to an approximate size of human kidney; however, the model did not have calyx structure, inside of the model which was empty. The pressure was not increased the same as the in-vivo human tests. There may also be air leaks from the joints. The relatively slow increase in pressure may be result of these realities.

To evaluate the accuracy of the sensor and disposables, further experiments were performed. The second experiment setup was constituted with ex-vivo animal kidneys. In experiment of Schwalb et al. (1993), rising the flow rate of the hydraulic pump during ureteroscopy at a stable pressure resulted in increased by 13 to 40 cmH_2O when flow was increased from 120 to 200 cc per min at a constant pressure. The maximum IRP in 16 ex-vivo pig kidneys was 596 cmH_2O, at inflow pressures 300 mmHg. The renal rupture was produced by gradually increasing the inflow pressure above 300 mmHg. In this thesis, the sheep kidney was preferred. The sheep kidneys were significantly smaller than human kidney, however the calyx structure and tissue were more likely than 3D printed model. Since the sheep ureter is narrow, the ureteral access sheath cannot be inserted with sensor catheter simultaneously. That's why the ureters were dilated by dilator of ureteral access sheath. The flushing pump was utilized during monitoring; the pressure was increased by increasing the flow rate of the device. In all 6 kidneys, the critical level between Level 2 to 3 were reached with flow rate of 150 to 210 ml/min, respectively.

The flushing pump was not used in in-vivo human experiments due to high flow rates. The endourological procedure was performed with gravity-based irrigation. The irrigation flow was measured as 570 ml/min. However, the gravity-based system cannot reach irrigation pressure same as automatic pump. In our study, Dr. Gokce performed PCNL and the baseline pressure was 5 cmH_2O. The pressure was increased to 9 cmH_2O when manual irrigation was done. In this study, one in-vivo experiment was performed due to the sensors' stock limitations. The prices of the sensors were increased by 300% in Turkish market which cause decrease in the demand and effect the stock of the products.

In literature, in the study of Gokce et al. (2021), the effect of location of nephroscope and percutaneous sheath on intrarenal pressure was investigated. When the nephroscope was inside the sheath and the sheath located in the pelvis, the lowest IRP was observed. To confirm this fact, also relocation of the sheath and nephroscope was examined. The sheath was pulled back from nephroscope. The pressure increase was observed due to reduce of outflow. The outflow was supplied from the valves on the sheath. The pressure was ascended about to 30 cmH_2O. In study of Gokce et al. (2021), the mean pressure was 35 cmH_2O in the scope location. The effect of the active aspiration on system was also observed, the pressure was declined quickly.

Change of pressure due to irrigation flow rate change was also observed during the experiment. Thus, instead of nephroscope, FURS was inserted antegradely. The flexible scope had 3.6 Fr working channel and irrigation was sustained from the channel. The irrigation flow was diminished with narrower channel. The results showed that, the manual irrigation can be increased the pressure maximum of 16 cmH_2O.

5.2 Conclusion

At the beginning of the study, it was thought that a disposable ureteral catheter or ureteral access sheath with pressure monitoring feature, can be used for avoiding complications related to elevated intrarenal pressures in endourology. However, during the study, we kept in mind that different endourological procedures required different disposables. So that, 2 different disposables; a ureteral access sheath for RIRS and a ureteral catheter for PCNL were designed. A pressure sensor with 1Fr diameter was inserted to measure the pressure that should be kept under 40 cmH_2O. The increase of intrarenal pressure might have caused absorption of endotoxin or bacteria that may lead to fever and urosepsis.

3 setups were organized; a 3D printed kidney model, an ex-vivo animal and an in-vivo patient experiment. The results from these experiments showed that the disposables can be used for real time pressure monitoring during endourology. The disposable with sensor can be used mainly for critical patients with older age, cardiac disease, etc.

Current findings of the study also lead to future aspects of connecting the disposables with pressure sensors to an active irrigation pump that can alarm the surgeon when the maximum level was reached. Moreover, an irrigation flow system that work in coordinate with sensor can be achieved. The system can also adjust the irrigation flow according to real time pressure value that can be limited to maximum pressure value of 40 cmH_2O.

REFERENCES

Aboumarzouk, O. M., Kata, S. G., Keeley, F. X., McClinton, S., & Nabi, G. (2012). Extracorporeal shock wave lithotripsy (ESWL) versus ureteroscopic management for ureteric calculi. *Cochrane Database Syst Rev*(5), CD006029. https://doi.org/10.1002/14651858.CD006029.pub4

Akman, T., Binbay, M., Yuruk, E., Sari, E., Seyrek, M., Kaba, M., Berberoglu, Y., & Muslumanoglu, A. Y. (2011). Tubeless procedure is most important factor in reducing length of hospitalization after percutaneous nephrolithotomy: results of univariable and multivariable models. *Urology*, *77*(2), 299-304. https://doi.org/10.1016/j.urology.2010.06.060

Alivizatos, G., & Skolarikos, A. (2006). Is there still a role for open surgery in the management of renal stones? *Curr Opin Urol*, *16*(2), 106-111. https://doi.org/10.1097/01.mou.0000193379.08857.e7

Alsmadi, J., Fan, J., Zhu, W., Wen, Z., & Zeng, G. (2018). The Influence of Super-Mini Percutaneous Nephrolithotomy on Renal Pelvic Pressure In Vivo. *J Endourol*, *32*(9), 819-823. https://doi.org/10.1089/end.2018.0239

Alsyouf, M., Abourbih, S., West, B., Hodgson, H., & Baldwin, D. D. (2018). Elevated Renal Pelvic Pressures during Percutaneous Nephrolithotomy Risk Higher Postoperative Pain and Longer Hospital Stay. *J Urol*, *199*(1), 193-199. https://doi.org/10.1016/j.juro.2017.08.039

Anderson, J. C., JA. (2012). Surgical anatomy of the retroperitoneum, adrenals, kidneys, and ureters. In W. McDougal, Kavoussi, Novic, Partin, Ramchandani (Ed.), *Campbell-Walsh Urology* (Vol. 10, pp. 3-6). Saunders Elsevier.

Anonymous.(2009).*https://training.seer.cancer.gov/anatomy/urinary/components/kidney.html*.

Anonymous. (2020). *https://www.hopkinsmedicine.org/health/wellness-and-prevention/anatomy-of-the-urinary-system*. The Johns Hopkins University, The Johns Hopkins Hospital, and Johns Hopkins Health System.

Assimos, D., Krambeck, A., Miller, N. L., Monga, M., Murad, M. H., Nelson, C. P., Pace, K. T., Pais, V. M., Jr., Pearle, M. S., Preminger, G. M., Razvi, H., Shah, O., & Matlaga, B. R. (2016). Surgical Management of Stones: American Urological Association/Endourological Society Guideline, PART I. *J Urol*, *196*(4), 1153-1160. https://doi.org/10.1016/j.juro.2016.05.090

Bach, T., Geavlete, B., Herrmann, T. R., & Gross, A. J. (2008). Working tools in flexible ureterorenoscopy--influence on flow and deflection: what does matter? *J Endourol*, *22*(8), 1639-1643. https://doi.org/10.1089/end.2008.0184

Binbay, M., Yuruk, E., Akman, T., Ozgor, F., Seyrek, M., Ozkuvanci, U., Berberoglu, Y., & Muslumanoglu, A. Y. (2010). Is there a difference in outcomes between digital and fiberoptic flexible ureterorenoscopy procedures? *J Endourol*, *24*(12), 1929-1934. https://doi.org/10.1089/end.2010.0211

Caballero-Romeu, J. P., Galan-Llopis, J. A., Soria, F., Morcillo-Martin, E., Caballero-Perez, P., Garcia, A., De La Cruz-Conty, J. E., & Romero-Maroto, J. (2018). Micro-ureteroscopy vs. ureteroscopy: effects of miniaturization on renal vascularization and intrapelvic pressure. *World J Urol*, *36*(5), 811-817. https://doi.org/10.1007/s00345-018-2205-y

Cai, Y., Li, X., Zhu, B., Chen, R., Ye, C., Wang, Y., Wang, Y., Tao, Y., Sun, Q., & Wen, X. (2012). A practical pressure measuring method for the upper urinary tract during ureteroscopy. *Clin Invest Med*, *35*(5), E322. https://doi.org/ 10.25011/cim.v35i5.18705

Chung, B. S., GDBJ. . (2012). Anatomy of the lower urinary tract and male genitalia. In A. K. Wein, LR.; Novick, AC.; Partin, AW.; Peters, CA. (Ed.), *Campbell-Walsh Urology* (Vol. 10, pp. 59-60). Saunders Elsevier.

Coward, R. J., Peters, C. J., Duffy, P. G., Corry, D., Kellett, M. J., Choong, S., & van't Hoff, W. G. (2003). Epidemiology of paediatric renal stone disease in the UK. *Arch Dis Child*, *88*(11), 962-965. https://doi.org/10.1136/adc.88.11.962

Curhan, G. C., Willett, W. C., Knight, E. L., & Stampfer, M. J. (2004). Dietary factors and the risk of incident kidney stones in younger women: Nurses' Health Study II. *Arch Intern Med*, *164*(8), 885-891. https://doi.org/10.1001/archinte.164.8.885

Cybulski, P. A., Joo, H., & Honey, R. J. (2004). Ureteroscopy: anesthetic considerations. *Urol Clin North Am*, *31*(1), 43-47, viii. https://doi.org/ 10.1016/S0094-0143(03)00087-9

de Groat, W. C., & Yoshimura, N. (2001). Pharmacology of the lower urinary tract. *Annu Rev Pharmacol Toxicol*, *41*, 691-721. https://doi.org/ 10.1146/ annurev.pharmtox.41.1.691

Desai, J., Zeng, G., Zhao, Z., Zhong, W., Chen, W., & Wu, W. (2013). A novel technique of ultra-mini-percutaneous nephrolithotomy: introduction and an initial experience for treatment of upper urinary calculi less than 2 cm. *Biomed Res Int*, *2013*, 490793. https://doi.org/10.1155/2013/490793

Dickstein, R. J., Kreshover, J. E., Babayan, R. K., & Wang, D. S. (2010). Is a safety wire necessary during routine flexible ureteroscopy? *J Endourol*, *24*(10), 1589-1592. https://doi.org/10.1089/end.2010.0145

Doizi, S. (2021). Intrarenal Pressure: What Is Acceptable for Flexible Ureteroscopy and Percutaneous Nephrolithotomy? *Eur Urol Focus*, *7*(1), 31-33. https://doi.org/10.1016/j.euf.2021.01.010

Doizi, S., Letendre, J., Cloutier, J., Ploumidis, A., & Traxer, O. (2021). Continuous monitoring of intrapelvic pressure during flexible ureteroscopy using a sensor wire: a pilot study. *World J Urol*, *39*(2), 555-561. https://doi.org/10.1007/s00345-020-03216-w

El-Shaer, W., Kandeel, W., Abdel-Lateef, S., Torky, A., & Elshaer, A. (2019). Complete Ultrasound-guided Percutaneous Nephrolithotomy in Prone and Supine Positions: A Randomized Controlled Study. *Urology*, *128*, 31-37. https://doi.org/10.1016/j.urology.2019.03.004

Elbadawi, A. (1996). Functional anatomy of the organs of micturition. *Urol Clin North Am*, *23*(2), 177-210. https://doi.org/10.1016/s0094-0143(05)70304-9

Fernstrom, I., & Johansson, B. (1976). Percutaneous pyelolithotomy. A new extraction technique. *Scand J Urol Nephrol*, *10*(3), 257-259. https://doi.org/10.1080/21681805.1976.11882084

Finlayson, B., & Reid, F. (1978). The expectation of free and fixed particles in urinary stone disease. *Invest Urol*, *15*(6), 442-448. https://www.ncbi.nlm.nih.gov/pubmed/649291

Fowler, C. J., Griffiths, D., & de Groat, W. C. (2008). The neural control of micturition. *Nat Rev Neurosci*, *9*(6), 453-466. https://doi.org/10.1038/nrn2401

Ge, H., Zheng, X., Na, Y., Hou, X., Yu, C., Ding, W., Wang, Y., Yu, Z., & He, H. (2016). Bilateral Same-Session Ureteroscopy for Treatment of Ureteral Calculi: A Systematic Review and Meta-Analysis. *J Endourol*, *30*(11), 1169-1179. https://doi.org/10.1089/end.2016.0472

Geavlete, P., Georgescu, D., Nita, G., Mirciulescu, V., & Cauni, V. (2006). Complications of 2735 retrograde semirigid ureteroscopy procedures: a single-center experience. *J Endourol*, *20*(3), 179-185. https://doi.org/ 10.1089/end.2006.20.179

Geraghty, R., Abourmarzouk, O., Rai, B., Biyani, C. S., Rukin, N. J., & Somani, B. K. (2015). Evidence for Ureterorenoscopy and Laser Fragmentation (URSL) for Large Renal Stones in the Modern Era. *Curr Urol Rep*, *16*(8), 54. https://doi.org/10.1007/s11934-015-0529-3

Goble, N. M., & Hammonds, J. C. (1987). An in vitro study of intracavitary pressures during percutaneous nephrolithotomy. *Br J Urol*, *60*(4), 307-311. https://doi.org/10.1111/j.1464-410x.1987.tb04973.x

Gokce, M. I., Karaburun, M. C., Babayigit, M., Aydog, E., Akpinar, C., Suer, E., & Gulpinar, O. (2021). Effect of Active Aspiration and Sheath Location on Intrapelvic Pressure During Miniaturized Percutaneous Nephrolithotomy. *Urology*. https://doi.org/10.1016/j.urology.2020.12.028

Guohua, Z., Wen, Z., Xun, L., Wenzhong, C., Yongzhong, H., Zhaohui, H., Ming, L., & Kaijun, W. (2007). The influence of minimally invasive percutaneous nephrolithotomy on renal pelvic pressure in vivo. *Surg Laparosc Endosc Percutan Tech*, *17*(4), 307-310. https://doi.org/10.1097/SLE.0b013e31806e61f4

Hamano, S., Nakatsu, H., Suzuki, N., Tomioka, S., Tanaka, M., & Murakami, S. (2005). Kidney stone disease and risk factors for coronary heart disease. *Int J Urol*, *12*(10), 859-863. https://doi.org/10.1111/j.1442-2042.2005.01160.x

Hesse, A., Brandle, E., Wilbert, D., Kohrmann, K. U., & Alken, P. (2003). Study on the prevalence and incidence of urolithiasis in Germany comparing the years 1979 vs. 2000. *Eur Urol*, *44*(6), 709-713. https://doi.org/10.1016/s0302-2838(03)00415-9

Hickling, D. R., Sun, T. T., & Wu, X. R. (2015). Anatomy and Physiology of the Urinary Tract: Relation to Host Defense and Microbial Infection. *Microbiol Spectr*, *3*(4). https://doi.org/10.1128/microbiolspec.UTI-0016-2012

Hinman, F. (1928). Urology: The Clinical Significance of Pyelovenous Backflow. *Cal West Med*, *29*(2), 111. https://www.ncbi.nlm.nih.gov/pubmed/18740784

Hollingsworth, J. M., Rogers, M. A., Kaufman, S. R., Bradford, T. J., Saint, S., Wei, J. T., & Hollenbeck, B. K. (2006). Medical therapy to facilitate urinary stone passage: a meta-analysis. *Lancet*, *368*(9542), 1171-1179. https://doi.org/10.1016/S0140-6736(06)69474-9

Jung, H. U., Jakobsen, J. S., Frimodt-Moeller, P. C., & Osther, P. J. (2008). Irrigation with isoproterenol during ureterorenoscopy causes no systemic side-effects. *Scand J Urol Nephrol*, *42*(2), 158-163. https://doi.org/10.1080/00365590701570631

Khan, S. R., & Canales, B. K. (2015). Unified theory on the pathogenesis of Randall's plaques and plugs. *Urolithiasis*, *43 Suppl 1*, 109-123. https://doi.org/ 10.1007/s00240-014-0705-9

Khan, S. R., & Hackett, R. L. (1993). Role of organic matrix in urinary stone formation: an ultrastructural study of crystal matrix interface of calcium oxalate monohydrate stones. *J Urol*, *150*(1), 239-245. https://doi.org/10.1016/s0022-5347(17)35454-x

Khan, S. R., Pearle, M. S., Robertson, W. G., Gambaro, G., Canales, B. K., Doizi, S., Traxer, O., & Tiselius, H. G. (2016). Kidney stones. *Nat Rev Dis Primers*, *2*, 16008. https://doi.org/10.1038/nrdp.2016.8

Kim, S. C., Burns, E. K., Lingeman, J. E., Paterson, R. F., McAteer, J. A., & Williams, J. C., Jr. (2007). Cystine calculi: correlation of CT-visible structure, CT number, and stone morphology with fragmentation by shock wave lithotripsy. *Urol Res*, *35*(6), 319-324. https://doi.org/10.1007/s00240-007-0117-1

Kok, D. J., & Khan, S. R. (1994). Calcium oxalate nephrolithiasis, a free or fixed particle disease. *Kidney Int*, *46*(3), 847-854. https://doi.org/10.1038/ki.1994.341

Kukreja, R. A., Desai, M. R., Sabnis, R. B., & Patel, S. H. (2002). Fluid absorption during percutaneous nephrolithotomy: does it matter? *J Endourol*, *16*(4), 221-224. https://doi.org/10.1089/089277902753752160

L'Esperance J, O., Ekeruo, W. O., Scales, C. D., Jr., Marguet, C. G., Springhart, W. P., Maloney, M. E., Albala, D. M., & Preminger, G. M. (2005). Effect of ureteral access sheath on stone-free rates in patients undergoing ureteroscopic management of renal calculi. *Urology*, *66*(2), 252-255. https://doi.org/10.1016/j.urology.2005.03.019

Lahme, S., Bichler, K. H., Strohmaier, W. L., & Gotz, T. (2001). Minimally invasive PCNL in patients with renal pelvic and calyceal stones. *Eur Urol*, *40*(6), 619-624. https://doi.org/10.1159/000049847

Lamb, A. D., Vowler, S. L., Johnston, R., Dunn, N., & Wiseman, O. J. (2011). Meta-analysis showing the beneficial effect of alpha-blockers on ureteric stent discomfort. *BJU Int*, *108*(11), 1894-1902. https://doi.org/10.1111/j.1464-410X.2011.10170.x

Landman, J., Venkatesh, R., Ragab, M., Rehman, J., Lee, D. I., Morrissey, K. G., Monga, M., & Sundaram, C. P. (2002). Comparison of intrarenal pressure and irrigant flow during percutaneous nephroscopy with an indwelling ureteral catheter, ureteral occlusion balloon, and ureteral access sheath. *Urology*, *60*(4), 584-587. https://doi.org/10.1016/s0090-4295(02)01861-7

Leijte, J. A., Oddens, J. R., & Lock, T. M. (2008). Holmium laser lithotripsy for ureteral calculi: predictive factors for complications and success. *J Endourol*, *22*(2), 257-260. https://doi.org/10.1089/end.2007.0299

Leusmann, D. B., Blaschke, R., & Schmandt, W. (1990). Results of 5,035 stone analyses: a contribution to epidemiology of urinary stone disease. *Scand J Urol Nephrol*, *24*(3), 205-210. https://doi.org/10.3109/00365599009180859

Loftus, C. J., Hinck, B., Makovey, I., Sivalingam, S., & Monga, M. (2018). Mini Versus Standard Percutaneous Nephrolithotomy: The Impact of Sheath Size on Intrarenal Pelvic Pressure and Infectious Complications in a Porcine Model. *J Endourol*, *32*(4), 350-353. https://doi.org/10.1089/end.2017.0602

Low, R. K. (1999). Nephroscopy sheath characteristics and intrarenal pelvic pressure: human kidney model. *J Endourol*, *13*(3), 205-208. https://doi.org/10.1089/end.1999.13.205

Macarak, E. J., & Howard, P. S. (1999). The role of collagen in bladder filling. *Adv Exp Med Biol*, *462*, 215-223; discussion 225-233. https://doi.org/10.1007/978-1-4615-4737-2_17

Mager, R., Balzereit, C., Reiter, M., Gust, K., Borgmann, H., Husch, T., Nagele, U., Haferkamp, A., & Schilling, D. (2015). Introducing a Novel In Vitro Model to Characterize Hydrodynamic Effects of Percutaneous Nephrolithotomy Systems. *J Endourol*, *29*(8), 929-932. https://doi.org/10.1089/end.2014.0854

McKee, M. D., Nanci, A., & Khan, S. R. (1995). Ultrastructural immunodetection of osteopontin and osteocalcin as major matrix components of renal calculi. *J Bone Miner Res*, *10*(12), 1913-1929. https://doi.org/10.1002/jbmr.5650101211

Medical, S. o. B. (2014). Medical gallery of Blausen Medical 2014 [Figure Article]. *WikiJournal of Medicine*, *1*. https://doi.org/10.15347/wjm/2014.010

Michel, M. S., Honeck, P., & Alken, P. (2008). Conventional high pressure versus newly developed continuous-flow ureterorenoscope: urodynamic pressure evaluation of the renal pelvis and flow capacity. *J Endourol*, *22*(5), 1083-1085. https://doi.org/10.1089/end.2008.0016

Monga, M., Bodie, J., & Ercole, B. (2004). Is there a role for small-diameter ureteral access sheaths? Impact on irrigant flow and intrapelvic pressures. *Urology*, *64*(3), 439-441; discussion 441-432. https://doi.org/10.1016/ j.urology. 2004.04.060

Muller-Mattheis, V. G., Schmale, D., Seewald, M., Rosin, H., & Ackermann, R. (1991). Bacteremia during extracorporeal shock wave lithotripsy of renal calculi. *J Urol*, *146*(3), 733-736. https://doi.org/10.1016/s0022-5347(17)37908-9

Ordon, M., Urbach, D., Mamdani, M., Saskin, R., RJ, D. A. H., & Pace, K. T. (2014). The surgical management of kidney stone disease: a population based time series analysis. *J Urol*, *192*(5), 1450-1456. https://doi.org/ 10.1016/j.juro.2014.05.095

Osman, M., Wendt-Nordahl, G., Heger, K., Michel, M. S., Alken, P., & Knoll, T. (2005). Percutaneous nephrolithotomy with ultrasonography-guided renal access: experience from over 300 cases. *BJU Int*, *96*(6), 875-878. https://doi.org/10.1111/j.1464-410X.2005.05749.x

Pace, K. T., Ghiculete, D., Harju, M., Honey, R. J., & University of Toronto Lithotripsy, A. (2005). Shock wave lithotripsy at 60 or 120 shocks per minute: a randomized, double-blind trial. *J Urol*, *174*(2), 595-599. https://doi.org/10.1097/01.ju.0000165156.90011.95

Pace, K. T., Kroczak, T., Wijnstok, N. J., Kamphuis, G. M., Esen, T., Toutziaris, C., Silva, B., & de la Rosette, J. J. (2017). Same Session Bilateral Ureteroscopy for Multiple Stones: Results from the CROES URS Global Study. *J Urol*, *198*(1), 130-137. https://doi.org/10.1016/j.juro.2017.01.074

Park, J. M., Bloom, D. A., & McGuire, E. J. (1997). The guarding reflex revisited. *Br J Urol*, *80*(6), 940-945. https://doi.org/10.1046/j.1464-410x.1997.00488.x

Pearle, M. S., Lingeman, J. E., Leveillee, R., Kuo, R., Preminger, G. M., Nadler, R. B., Macaluso, J., Monga, M., Kumar, U., Dushinski, J., Albala, D. M., Wolf, J. S., Jr., Assimos, D., Fabrizio, M., Munch, L. C., Nakada, S. Y., Auge, B., Honey, J., Ogan, K., Pattaras, J., McDougall, E. M., Averch, T. D., Turk, T., Pietrow, P., & Watkins, S. (2005). Prospective, randomized trial comparing shock wave lithotripsy and ureteroscopy for lower pole caliceal calculi 1 cm or less. *J Urol*, *173*(6), 2005-2009. https://doi.org/10.1097/01.ju.0000158458.51706.56

Pearle, M. S., Nadler, R., Bercowsky, E., Chen, C., Dunn, M., Figenshau, R. S., Hoenig, D. M., McDougall, E. M., Mutz, J., Nakada, S. Y., Shalhav, A. L., Sundaram, C., Wolf, J. S., Jr., & Clayman, R. V. (2001). Prospective randomized trial comparing shock wave lithotripsy and ureteroscopy for management of distal ureteral calculi. *J Urol*, *166*(4), 1255-1260. https://www.ncbi.nlm.nih.gov/pubmed/11547053

Perez Castro, E., Osther, P. J., Jinga, V., Razvi, H., Stravodimos, K. G., Parikh, K., Kural, A. R., de la Rosette, J. J., & Group, C. U. G. S. (2014). Differences in ureteroscopic stone treatment and outcomes for distal, mid-, proximal, or multiple ureteral locations: the Clinical Research Office of the Endourological Society ureteroscopy global study. *Eur Urol*, *66*(1), 102-109. https://doi.org/10.1016/j.eururo.2014.01.011

Pierre, S., & Preminger, G. M. (2007). Holmium laser for stone management. *World J Urol*, *25*(3), 235-239. https://doi.org/10.1007/s00345-007-0162-y

Pradere, B., Doizi, S., Proietti, S., Brachlow, J., & Traxer, O. (2018). Evaluation of Guidelines for Surgical Management of Urolithiasis. *J Urol*, *199*(5), 1267-1271. https://doi.org/10.1016/j.juro.2017.11.111

Preminger, G. M., Clayman, R. V., Hardeman, S. W., Franklin, J., Curry, T., & Peters, P. C. (1985). Percutaneous nephrostolithotomy vs open surgery for renal calculi. A comparative study. *JAMA*, *254*(8), 1054-1058. https://www.ncbi.nlm.nih.gov/pubmed/4021044

Ramey, S. L., Franke, W. D., & Shelley, M. C., 2nd. (2004). Relationship among risk factors for nephrolithiasis, cardiovascular disease, and ethnicity: focus on a law enforcement cohort. *AAOHN J*, *52*(3), 116-121. https://www.ncbi.nlm.nih.gov/pubmed/15068102

Rawandale-Patil, A. V., Ganpule, A. P., & Patni, L. G. (2019). Development of an innovative intrarenal pressure regulation system for mini-PCNL: A preliminary study. *Indian J Urol*, *35*(3), 197-201. https://doi.org/10.4103/iju.IJU_261_18

Ray, A. A., Ghiculete, D., Pace, K. T., & Honey, R. J. (2010). Limitations to ultrasound in the detection and measurement of urinary tract calculi. *Urology*, *76*(2), 295-300. https://doi.org/10.1016/j.urology.2009.12.015

Rehman, J., Monga, M., Landman, J., Lee, D. I., Felfela, T., Conradie, M. C., Srinivas, R., Sundaram, C. P., & Clayman, R. V. (2003). Characterization of intrapelvic pressure during ureteropyeloscopy with ureteral access sheaths. *Urology*, *61*(4), 713-718. https://doi.org/10.1016/s0090-4295(02)02440-8

Robertson, W. G., Peacock, M., & Nordin, B. E. (1971). Calcium oxalate crystalluria and urine saturation in recurrent renal stone-formers. *Clin Sci*, *40*(5), 365-374. https://doi.org/10.1042/cs0400365

Ruhayel, Y., Tepeler, A., Dabestani, S., MacLennan, S., Petrik, A., Sarica, K., Seitz, C., Skolarikos, A., Straub, M., Turk, C., Yuan, Y., & Knoll, T. (2017). Tract Sizes in Miniaturized Percutaneous Nephrolithotomy: A Systematic Review from the European Association of Urology Urolithiasis Guidelines Panel. *Eur Urol*, *72*(2), 220-235. https://doi.org/10.1016/j.eururo.2017.01.046

Saltzman, B., Khasidy, L. R., & Smith, A. D. (1987). Measurement of renal pelvis pressures during endourologic procedures. *Urology*, *30*(5), 472-474. https://doi.org/10.1016/0090-4295(87)90384-0

Santiago, J. E., Hollander, A. B., Soni, S. D., Link, R. E., & Mayer, W. A. (2017). To Dust or Not To Dust: a Systematic Review of Ureteroscopic Laser Lithotripsy Techniques. *Curr Urol Rep*, *18*(4), 32. https://doi.org/10.1007/s11934-017-0677-8

Scales, C. D., Jr., Lai, J. C., Dick, A. W., Hanley, J. M., van Meijgaard, J., Setodji, C. M., Saigal, C. S., & Urologic Diseases in America, P. (2014). Comparative effectiveness of shock wave lithotripsy and ureteroscopy for treating patients with kidney stones. *JAMA Surg*, *149*(7), 648-653. https://doi.org/10.1001/jamasurg.2014.336

Schwalb, D. M., Eshghi, M., Davidian, M., & Franco, I. (1993). Morphological and physiological changes in the urinary tract associated with ureteral dilation and ureteropyeloscopy: an experimental study. *J Urol*, *149*(6), 1576-1585. https://doi.org/10.1016/s0022-5347(17)36456-x

Seitz, C., Liatsikos, E., Porpiglia, F., Tiselius, H. G., & Zwergel, U. (2009). Medical therapy to facilitate the passage of stones: what is the evidence? *Eur Urol*, *56*(3), 455-471. https://doi.org/10.1016/j.eururo.2009.06.012

Semins, M. J., Trock, B. J., & Matlaga, B. R. (2008). The effect of shock wave rate on the outcome of shock wave lithotripsy: a meta-analysis. *J Urol*, *179*(1), 194-197; discussion 197. https://doi.org/10.1016/j.juro.2007.08.173

Shao, Y., Shen, Z. J., Zhu, Y. Y., Sun, X. W., Lu, J., & Xia, S. J. (2012). Fluid-electrolyte and renal pelvic pressure changes during ureteroscopic lithotripsy. *Minim Invasive Ther Allied Technol, 21*(4), 302-306. https://doi.org/10.3109/13645706.2011.595419

Skolarikos, A., Straub, M., Knoll, T., Sarica, K., Seitz, C., Petrik, A., & Turk, C. (2015). Metabolic evaluation and recurrence prevention for urinary stone patients: EAU guidelines. *Eur Urol*, *67*(4), 750-763. https://doi.org/10.1016/j.eururo.2014.10.029

Smith-Bindman, R., Aubin, C., Bailitz, J., Bengiamin, R. N., Camargo, C. A., Jr., Corbo, J., Dean, A. J., Goldstein, R. B., Griffey, R. T., Jay, G. D., Kang, T. L., Kriesel, D. R., Ma, O. J., Mallin, M., Manson, W., Melnikow, J., Miglioretti, D. L., Miller, S. K., Mills, L. D., Miner, J. R., Moghadassi, M., Noble, V. E., Press, G. M., Stoller, M. L., Valencia, V. E., Wang, J., Wang, R. C., & Cummings, S. R. (2014). Ultrasonography versus computed tomography for suspected nephrolithiasis. *N Engl J Med*, *371*(12), 1100-1110. https://doi.org/10.1056/NEJMoa1404446

Standring, S. (2008a). The anatomical basis of clinical practice. In *Gray's Anatomy* (Vol. 40). Churchill Livingstone Elsevier.

Standring, S. (2008b). Kidneys and ureter. In *Gray's Anatomy* (40 ed., pp. 1230–1231). Churchill Livingstone Elsevier.

Stenberg, A., Bohman, S. O., Morsing, P., Muller-Suur, C., Olsen, L., & Persson, A. E. (1988). Back-leak of pelvic urine to the bloodstream. *Acta Physiol Scand*, *134*(2), 223-234. https://doi.org/10.1111/j.1748-1716.1988.tb08483.x

Stern, J. M., Yiee, J., & Park, S. (2007). Safety and efficacy of ureteral access sheaths. *J Endourol*, *21*(2), 119-123. https://doi.org/10.1089/end.2007.9997

Suh, L. K., Rothberg, M. B., Landman, J., Katsumi, H., & Gupta, M. (2010). Intrarenal pressures generated during deployment of various antiretropulsion devices in an ex vivo porcine model. *J Endourol*, *24*(7), 1165-1168. https://doi.org/10.1089/end.2010.0118

Taylor, E. N., Stampfer, M. J., & Curhan, G. C. (2004). Dietary factors and the risk of incident kidney stones in men: new insights after 14 years of follow-up. *J Am Soc Nephrol*, *15*(12), 3225-3232. https://doi.org/10.1097/01.ASN. 0000146012.44570.20

Tepeler, A., Akman, T., Silay, M. S., Akcay, M., Ersoz, C., Kalkan, S., Armagan, A., & Sarica, K. (2014). Comparison of intrarenal pelvic pressure during micro-percutaneous nephrolithotomy and conventional percutaneous nephrolithotomy. *Urolithiasis*, *42*(3), 275-279. https://doi.org/10.1007/s00240-014-0646-3

Tokas, T., Herrmann, T. R. W., Skolarikos, A., Nagele, U., Training, Research in Urological, S., & Technology, G. (2019). Pressure matters: intrarenal pressures during normal and pathological conditions, and impact of increased values to renal physiology. *World J Urol*, *37*(1), 125-131. https://doi.org/10.1007/s00345-018-2378-4

Tokas, T., Skolarikos, A., Herrmann, T. R. W., Nagele, U., Training, Research in Urological, S., & Technology, G. (2019). Pressure matters 2: intrarenal pressure ranges during upper-tract endourological procedures. *World J Urol*, *37*(1), 133-142. https://doi.org/10.1007/s00345-018-2379-3

Trinchieri, A. (1996). Epidemiology of urolithiasis. *Arch Ital Urol Androl*, *68*(4), 203-249. https://www.ncbi.nlm.nih.gov/pubmed/8936716

Trinchieri, A. (2008). Epidemiology of urolithiasis: an update. *Clin Cases Miner Bone Metab*, *5*(2), 101-106. https://www.ncbi.nlm.nih.gov/pubmed/22460989

Troxel, S. A., & Low, R. K. (2002). Renal intrapelvic pressure during percutaneous nephrolithotomy and its correlation with the development of postoperative fever. *J Urol*, *168*(4 Pt 1), 1348-1351. https://doi.org/10.1097/ 01.ju.0000030996. 64339.f1

Turk, C., Petrik, A., Sarica, K., Seitz, C., Skolarikos, A., Straub, M., & Knoll, T. (2016). EAU Guidelines on Interventional Treatment for Urolithiasis. *Eur Urol*, *69*(3), 475-482. https://doi.org/10.1016/j.eururo.2015.07.041

Turney, B. W., Reynard, J. M., Noble, J. G., & Keoghane, S. R. (2012). Trends in urological stone disease. *BJU Int*, *109*(7), 1082-1087. https://doi.org/10.1111/ j.1464-410X.2011.10495.x

Violette, P. D., Cartwright, R., Briel, M., Tikkinen, K. A., & Guyatt, G. H. (2016). Guideline of guidelines: thromboprophylaxis for urological surgery. *BJU Int*, *118*(3), 351-358. https://doi.org/10.1111/bju.13496

Weblogographic.com. (2019). *Mesane ve böbrek arasındaki fark*.

Wendt-Nordahl, G., Mut, T., Krombach, P., Michel, M. S., & Knoll, T. (2011). Do new generation flexible ureterorenoscopes offer a higher treatment success than their predecessors? *Urol Res*, *39*(3), 185-188. https://doi.org/10.1007/s00240-010-0331-0

Wignall, G. R., Canales, B. K., Denstedt, J. D., & Monga, M. (2008). Minimally invasive approaches to upper urinary tract urolithiasis. *Urol Clin North Am*, *35*(3), 441-454, viii. https://doi.org/10.1016/j.ucl.2008.05.004

Wimpissinger, F., Turk, C., Kheyfets, O., & Stackl, W. (2007). The silence of the stones: asymptomatic ureteral calculi. *J Urol*, *178*(4 Pt 1), 1341-1344; discussion 1344. https://doi.org/10.1016/j.juro.2007.05.128

Wu, C., Hua, L. X., Zhang, J. Z., Zhou, X. R., Zhong, W., & Ni, H. D. (2017). Comparison of renal pelvic pressure and postoperative fever incidence between standard- and mini-tract percutaneous nephrolithotomy. *Kaohsiung J Med Sci*, *33*(1), 36-43. https://doi.org/10.1016/j.kjms.2016.10.012

Zhong, W., Zeng, G., Wu, K., Li, X., Chen, W., & Yang, H. (2008). Does a smaller tract in percutaneous nephrolithotomy contribute to high renal pelvic pressure and postoperative fever? *J Endourol*, *22*(9), 2147-2151. https://doi.org/10.1089/end.2008.0001

Zhu, W., Li, J., Yuan, J., Liu, Y., Wan, S. P., Liu, G., Chen, W., Wu, W., Luo, J., Zhong, D., Qi, D., Lei, M., Zhong, W., Zhang, Z., He, Z., Zhao, Z., Lu, S., Wu, Y., & Zeng, G. (2017). A prospective and randomised trial comparing fluoroscopic, total ultrasonographic, and combined guidance for renal access in mini-percutaneous nephrolithotomy. *BJU Int*, *119*(4), 612-618. https://doi.org/10.1111/bju.13703